Supporting Information

Dynamic Self-Inclusion Behavior of Pillar[5]arene-Based Pseudo[1]rotaxanes

Yangfan Guan[a], *Pingying Liu*[b], *Chao Deng*[a], *Mengfei Ni*[a], *Shuhan Xiong*[a], *Chen Lin*[a], *Xiaoyu Hu*[a]*, *Jing Ma*[b]*, *Leyong Wang*[a]*

[a] Key Laboratory of Mesoscopic Chemistry of MOE, Center for Multimolecular Chemistry, School of Chemistry and Chemical Engineering, Nanjing University, Nanjing 210093, China

[b] Institute of Theoretical and Computational Chemistry, Nanjing University, Nanjing 210093, China

Table of Contents

1. General methods

All solvents and reagents were used as supplied. The commercially available reagents and solvents were employed without further purification. All reactions were performed in atmosphere unless noted. Column chromatography was performed with silica gel (200 - 300 mesh) produced by Qingdao Marine Chemical Factory, Qingdao (China). All yields were given as isolated yields.

2. Measurements

Melting points (Mp) were determined using a Focus X-4 apparatus (made in China) and were not corrected. NMR spectra were recorded on a Bruker DPX 300 MHz spectrometer and Bruker DPX 400 MHz with internal standard tetramethylsilane (TMS) and solvent signals as internal references. Chemical shifts (δ) are reported in ppm downfield from tetramethylsilane. Low-resolution electrospray ionization mass spectra (LR-ESI-MS) were obtained on Finnigan Mat TSQ 7000 instruments. High-resolution electrospray ionization mass spectra (HR-ESI-MS) were recorded on an Agilent 6540Q-TOF LCMS equipped with an electrospray ionization (ESI) probe operating in positive-ion mode with direct infusion.

3. 2D COSY spectrum of $\mathbf{1}_{conf1}$

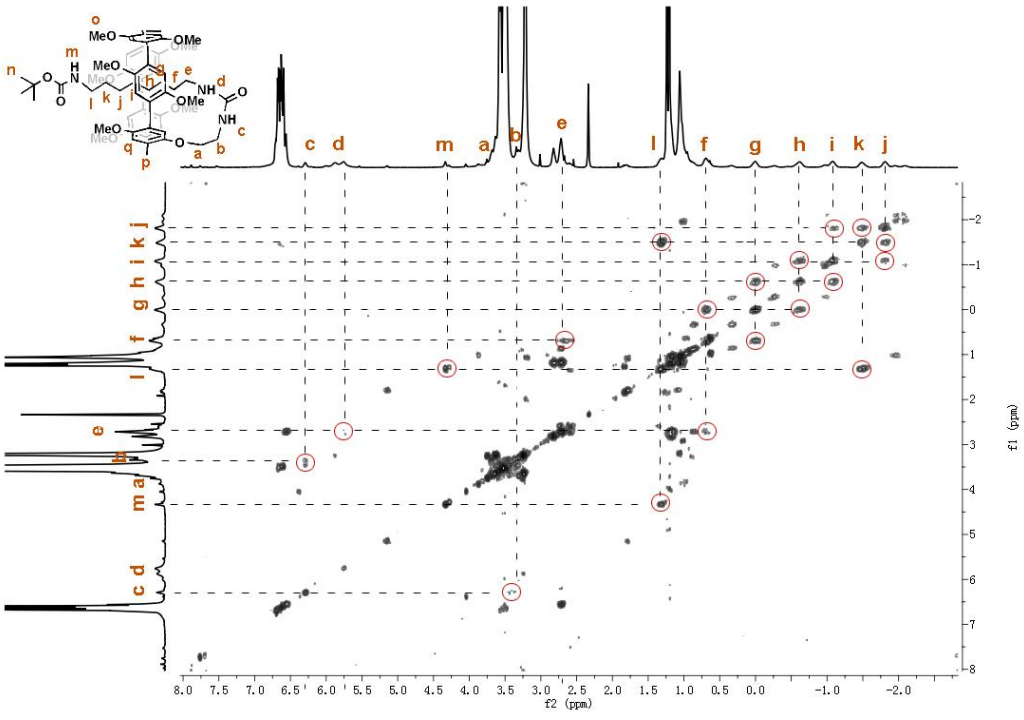

Figure S1. ^{1}H COSY spectrum (400 MHz, DMSO-d_6, 298 K) of compound $\mathbf{1}_{conf1}$ (This spectrum is obtained 24 h after compound $\mathbf{1}_{conf1}$ was separated, thus it showed a series of isomer peaks because of the dynamic property of $\mathbf{1}_{conf1}$, but still it can be utilized in the assignment for the protons of $\mathbf{1}_{conf1}$).

4. ^{1}H NMR spectra of $\mathbf{1}_{conf1}$ at multiple concentrations

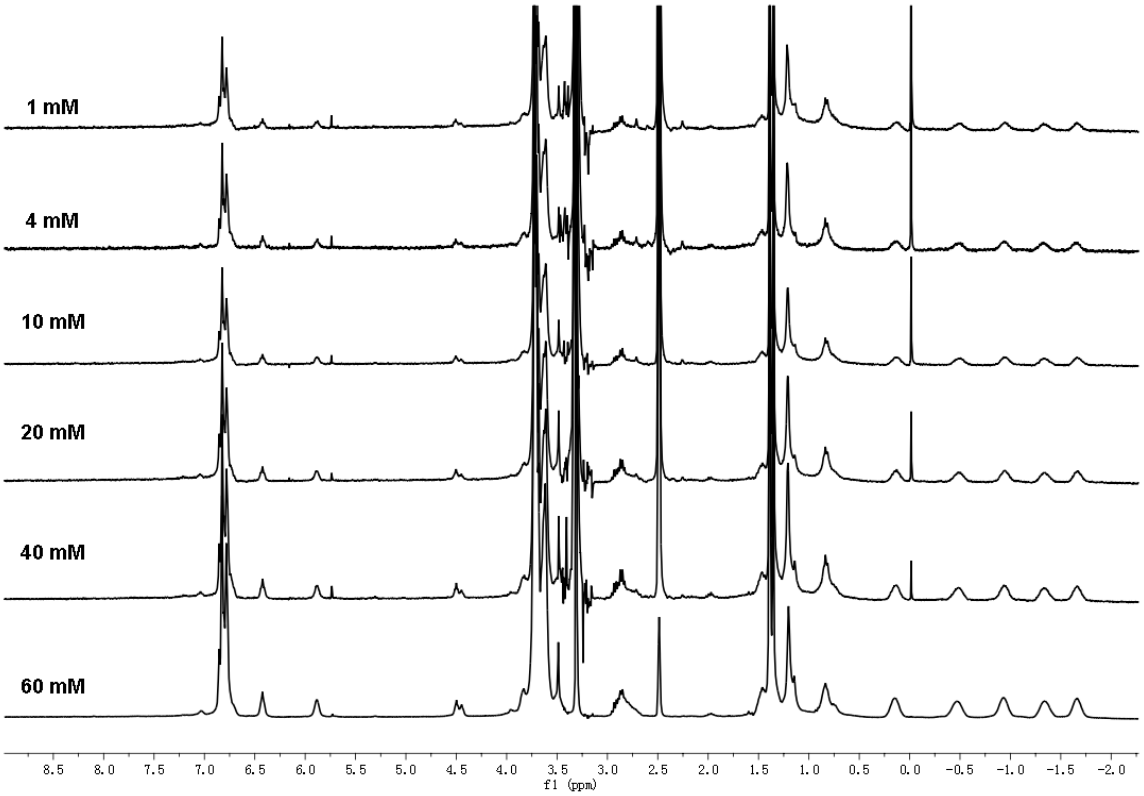

Figure S2. ^{1}H NMR spectra (400 MHz, DMSO-d_6, 298 K) of $\mathbf{1}_{conf1}$ at multiple concentrations.

5. Full 2D ROESY spectrum of $\mathbf{1}_{conf1}$ and 2

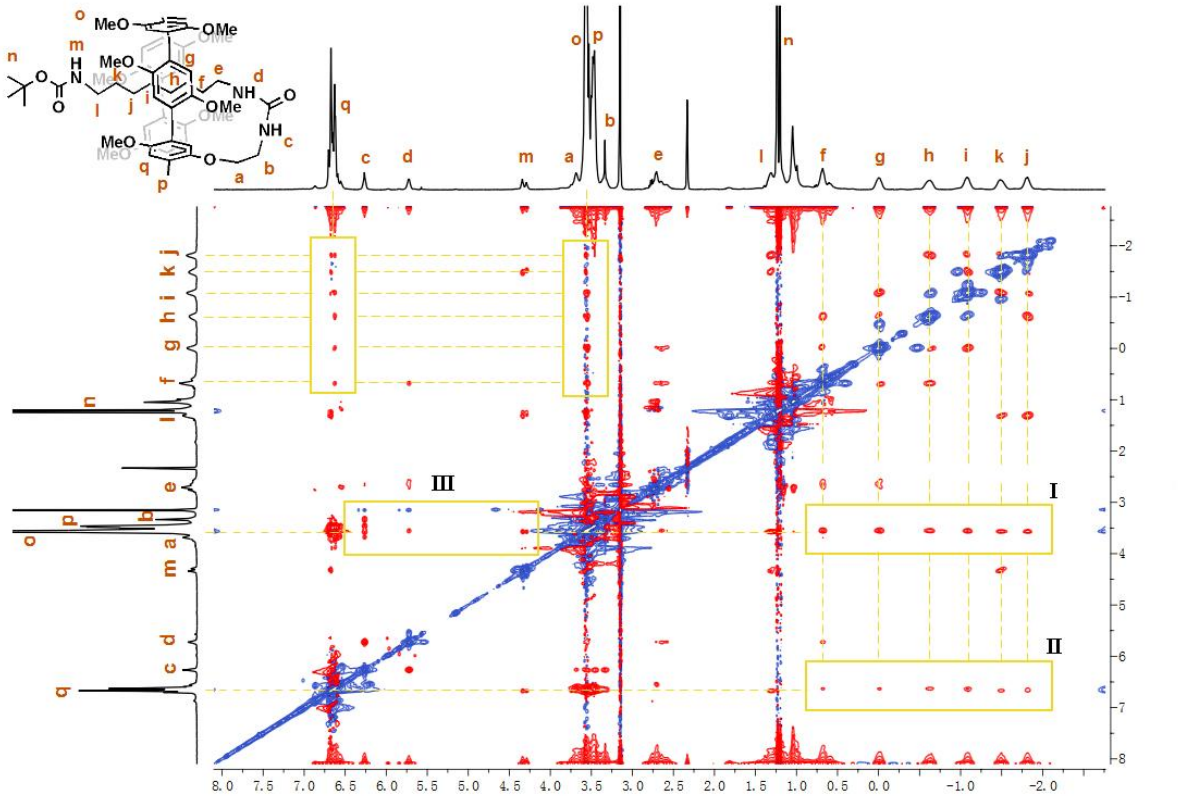

Figure S3. Full 2D ROESY NMR spectrum (400 MHz, DMSO-d_6, 298 K) of $\mathbf{1}_{conf1}$.

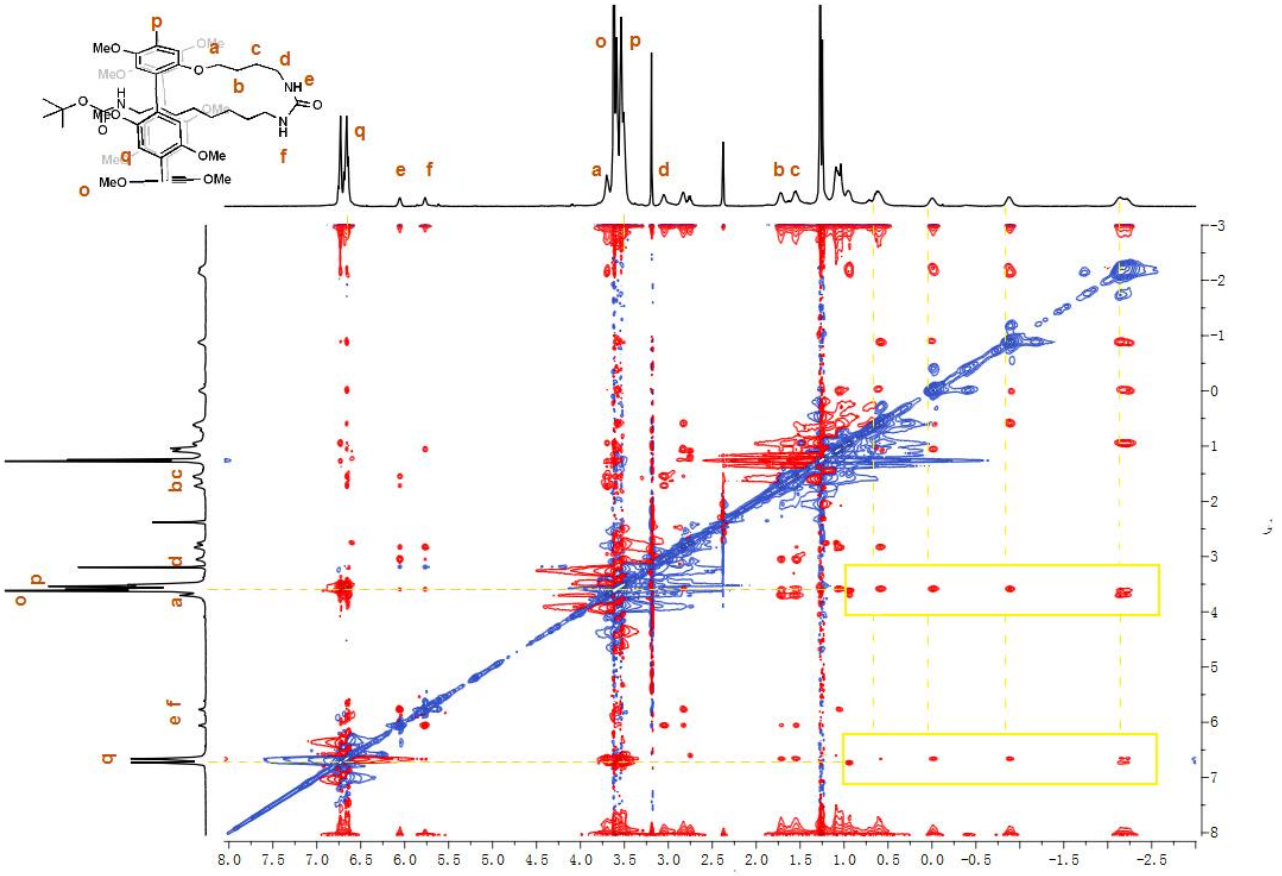

Figure S4. Full 2D ROESY NMR spectrum (400 MHz, DMSO-d_6, 298 K) of **2**.

6. Various concentration ^{1}H NMR spectra of 3

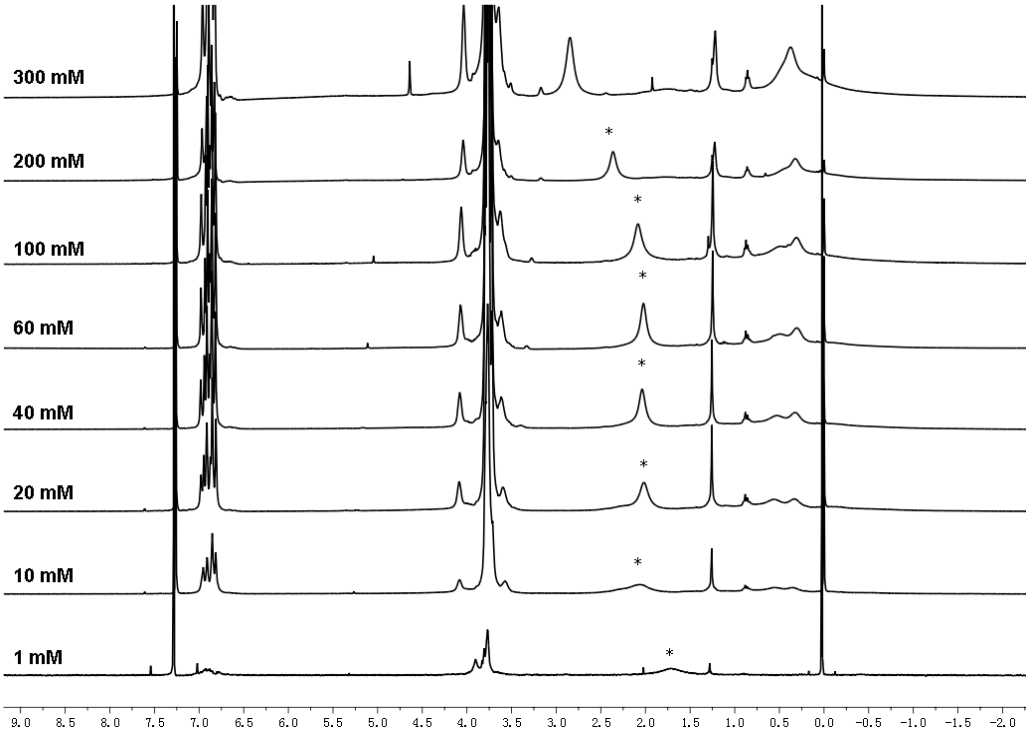

Figure S5. ^{1}H NMR spectra (400MHz, 298 K, $CDCl_3$) of **3** at various concentrations (The water peaks were labeled with * mark).

7. ^{1}H NMR spectra of 4 in different solvents

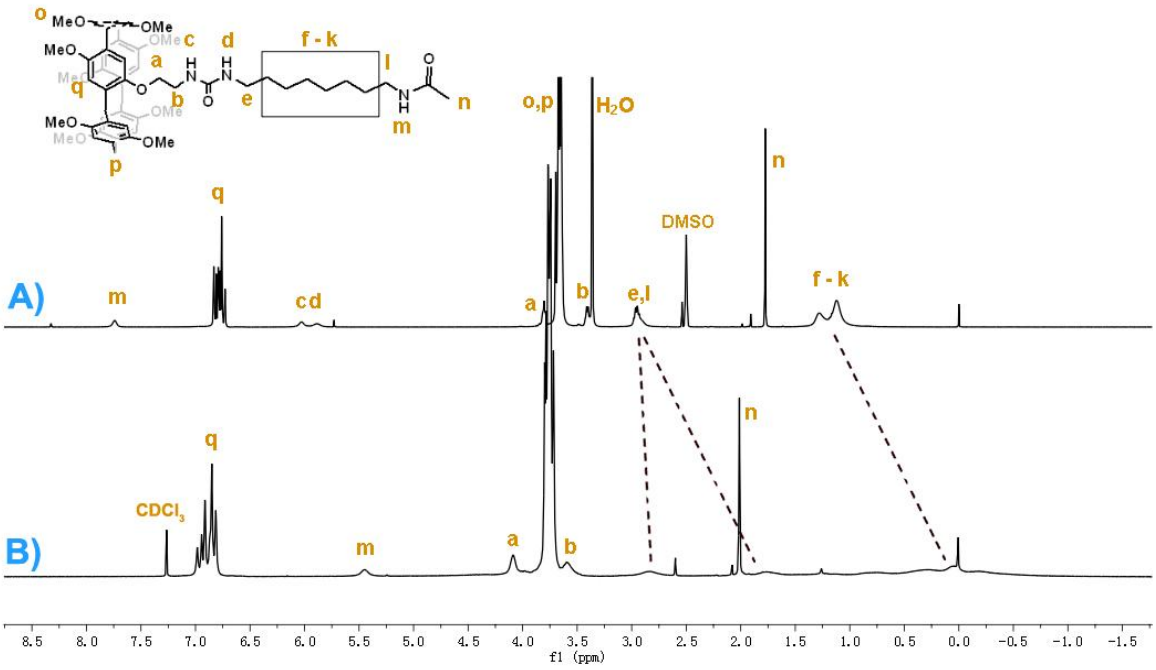

Figure S6. ^{1}H NMR spectra (400 MHz, 298 K) of **4** (A) in DMSO-d_6 and (B) in $CDCl_3$.

8. Partial 2D ROESY spectrum of 5

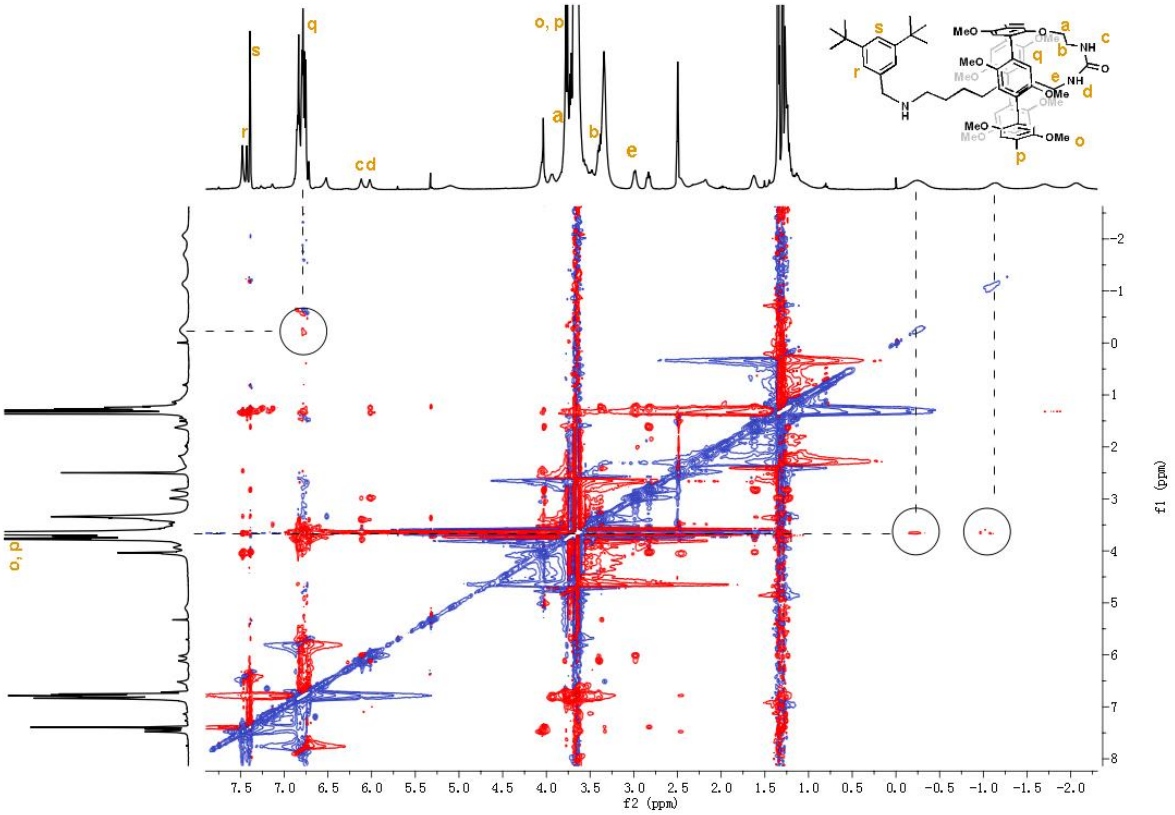

Figure S7. 2D ROESY NMR spectrum (400 MHz, DMSO-d_6, 298 K) of **5.**

9. Spontaneous and slow transformation from 2 to 2u in DMSO monitored by ^{1}H NMR spectra

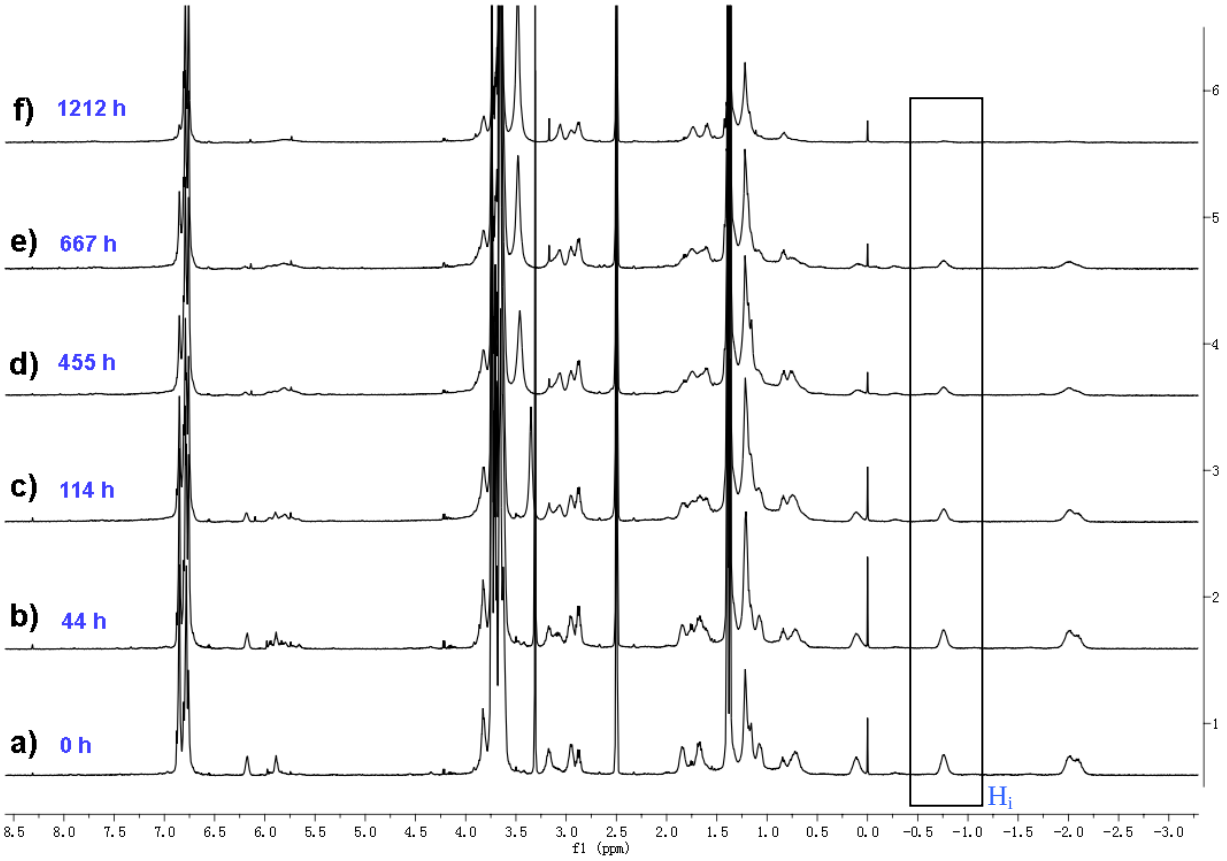

Figure S8. ^{1}H NMR spectra (400 MHz, DMSO-d_6, 298 K) of the time-dependent transformation of **2:** (a) compound **2**, (b) **2** after 44 h, (c) **2** after 114 h, (d) **2** after 455 h, (e) **2** after 667 h, and (f) **2** after 1212 h.

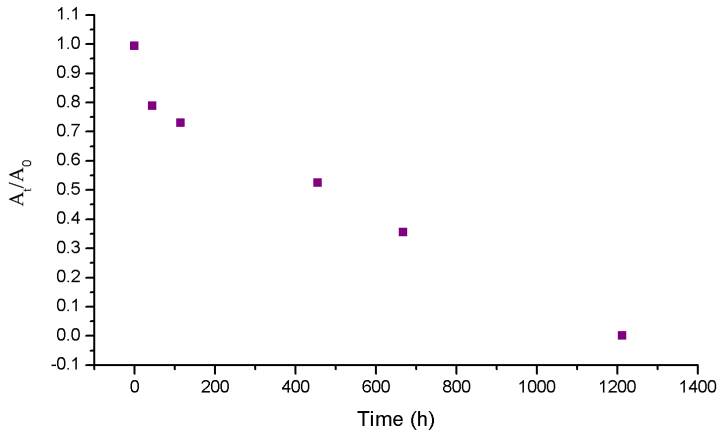

Figure S9. Intensity change of the threaded methylene proton H_i of **2** upon time in the dethreading process. A_0 is the initial integration of the selected peak H_i shown in Figure S9, A_t is the integration of the selected peak at time *t*.

10. Spectra (^{1}H, ^{13}C, and HRESIMS)

10.1 Compound $\mathbf{1}_{conf1}$ and **1u**

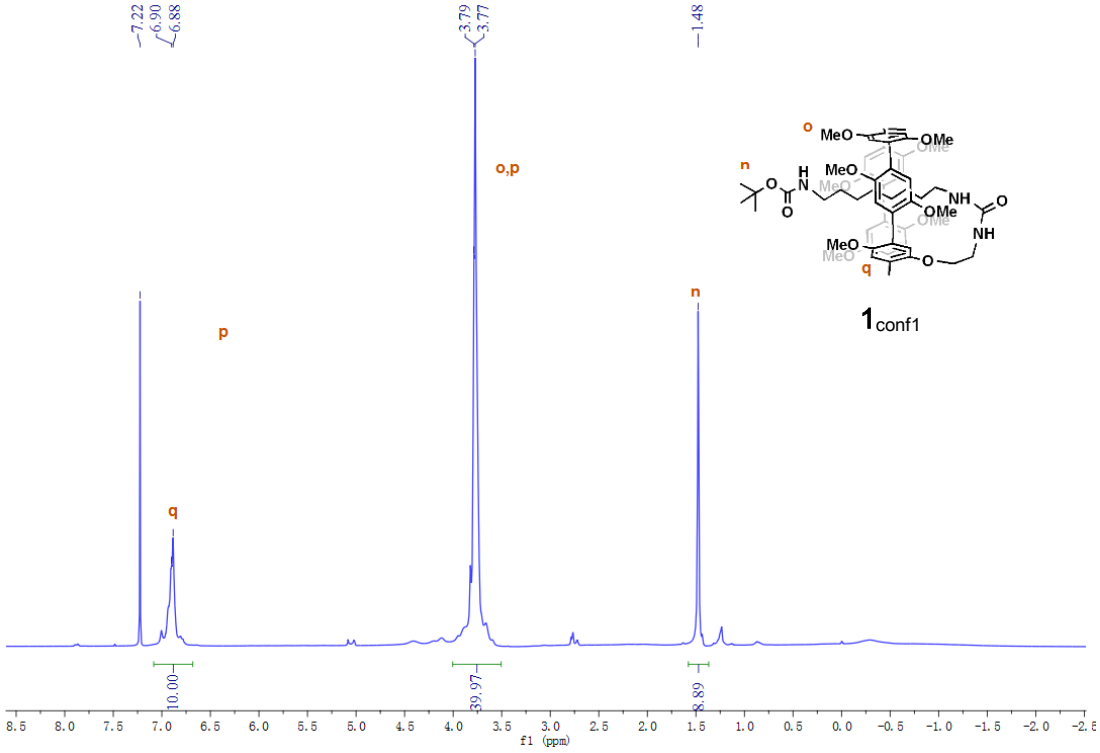

Figure S10. ^{1}H NMR spectrum (400 MHz, $CDCl_3$, 298 K) of compound $\mathbf{1}_{conf1}$.

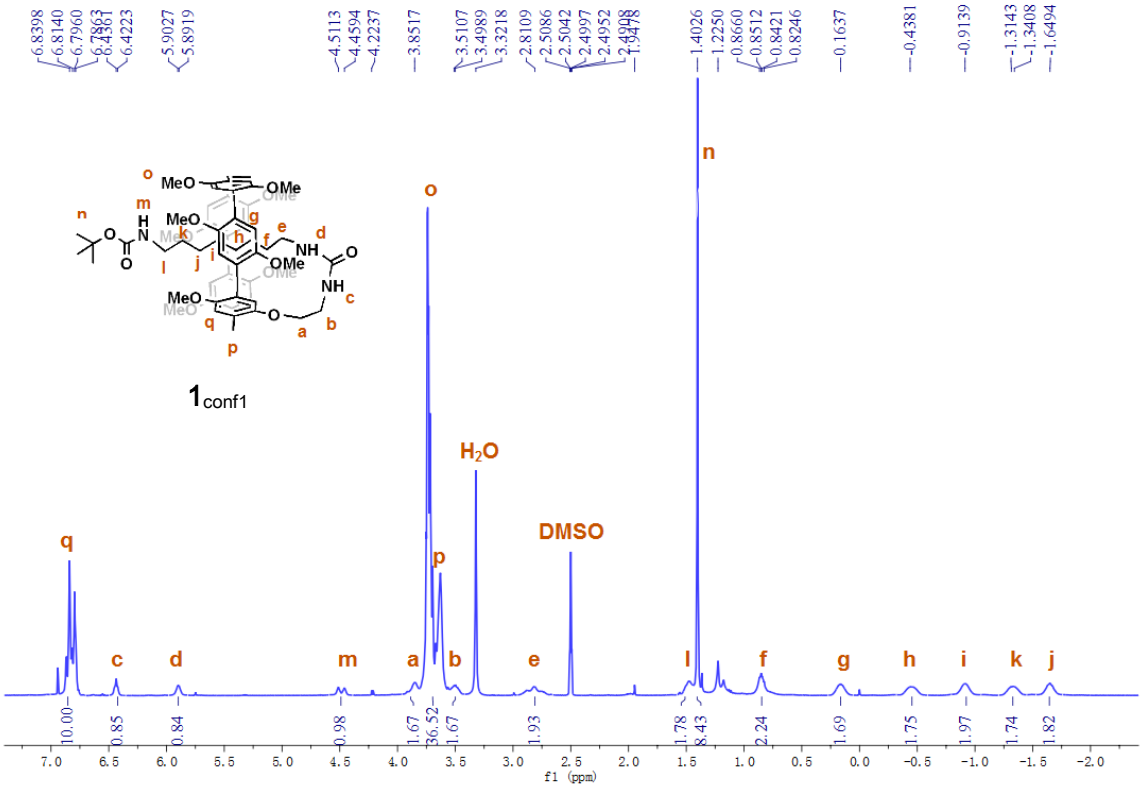

Figure S11. ^{1}H NMR spectrum (400 MHz, DMSO-d_6, 298 K) of compound $\mathbf{1}_{conf1}$.

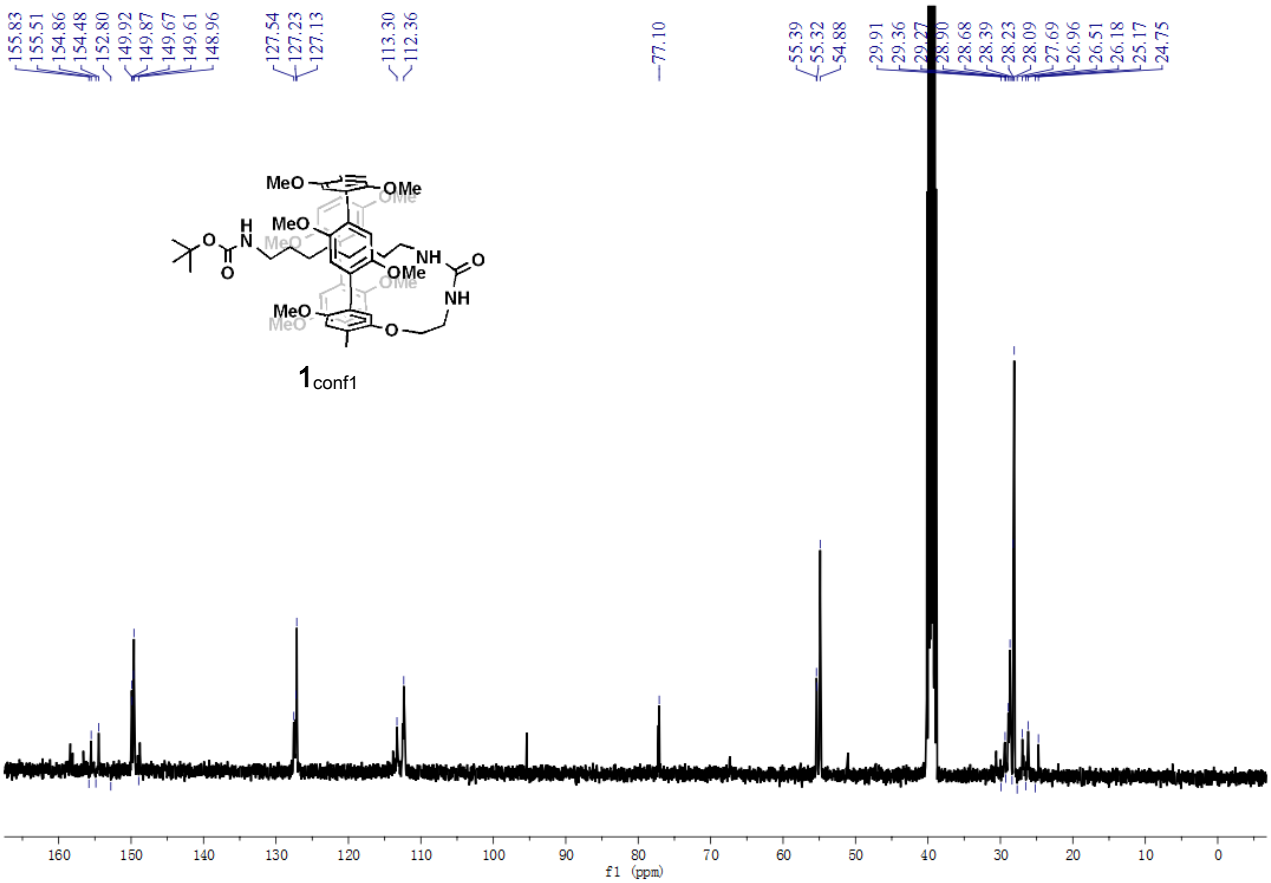

Figure S12. ^{13}C NMR spectrum (100 MHz, DMSO-d_6, 298 K) of compound **1**$_{conf1}$.

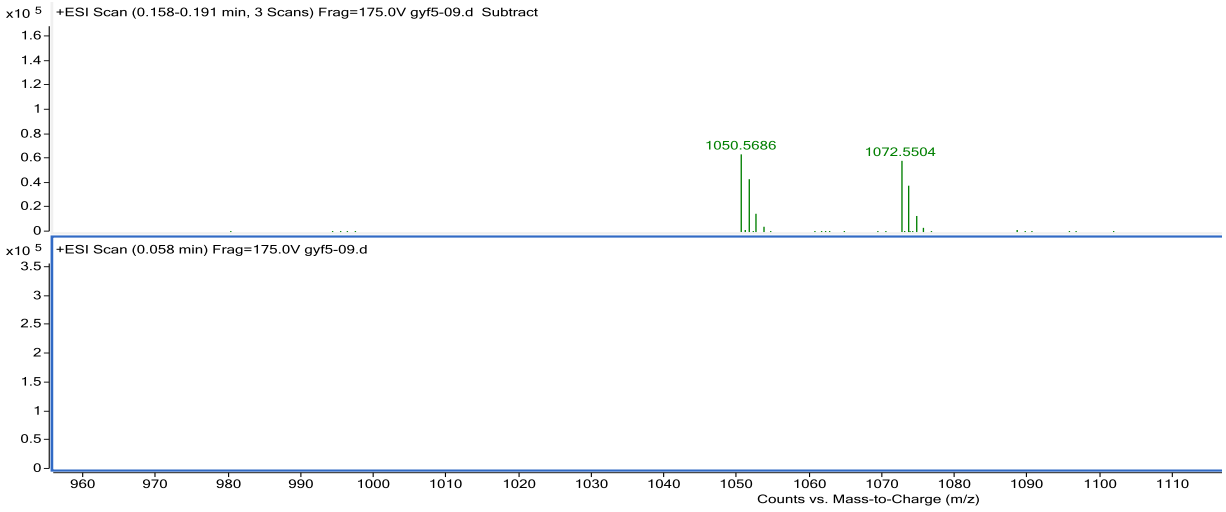

Figure S13. High resolution electrospray ionization mass spectrum of **1**$_{conf1}$.

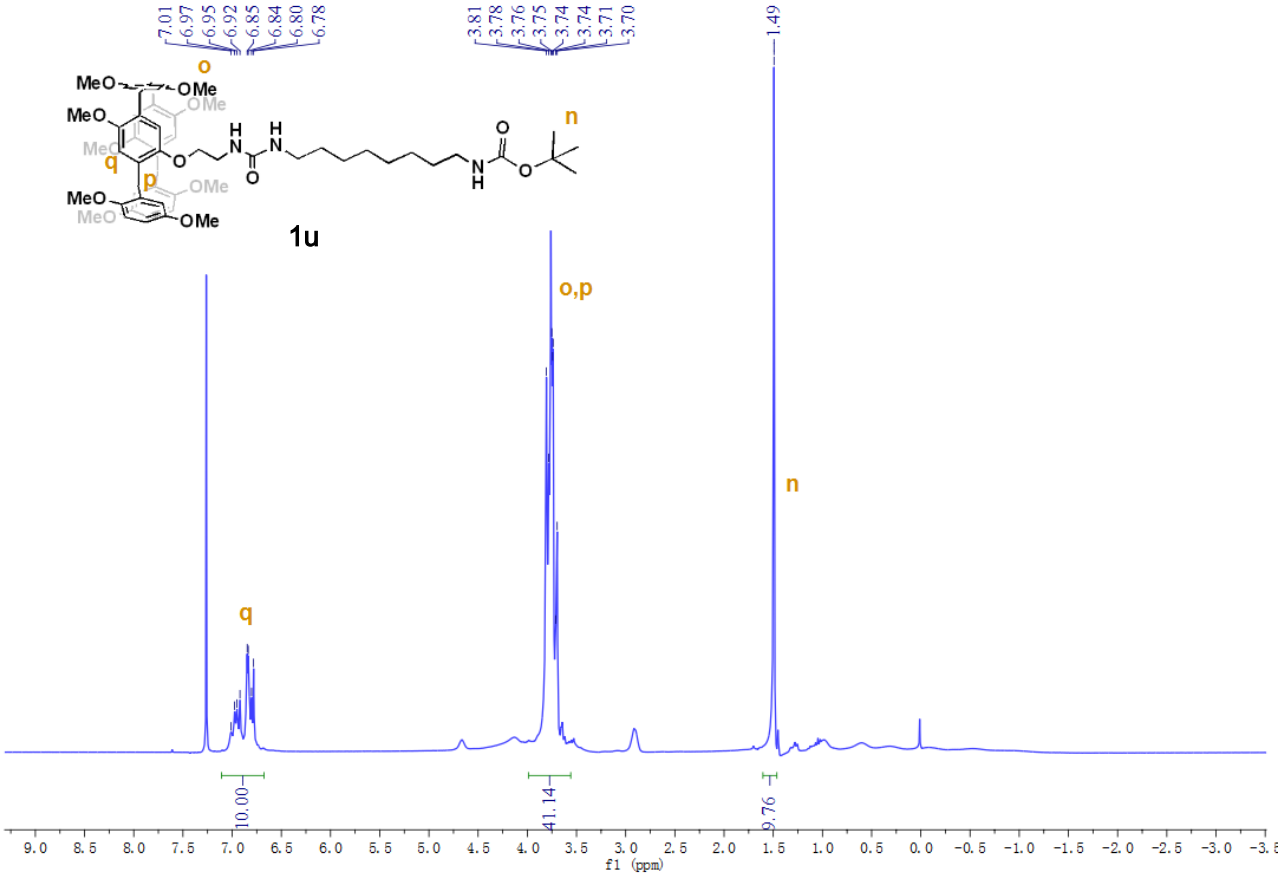

Figure S14. ^{1}H NMR spectrum (400 MHz, $CDCl_3$, 298 K) of compound **1u.**

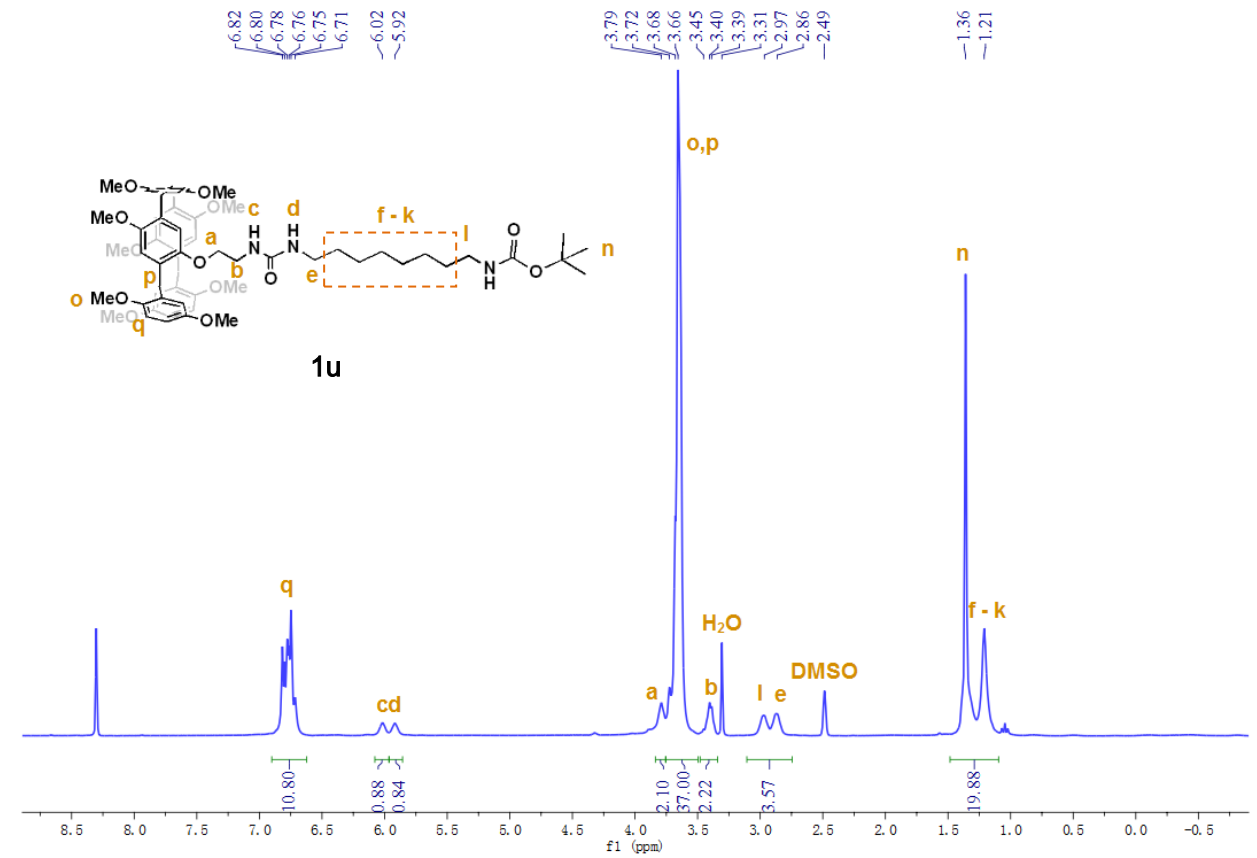

Figure S15. ^{1}H NMR spectrum (400 MHz, DMSO-d_6, 298 K) of compound **1u.**

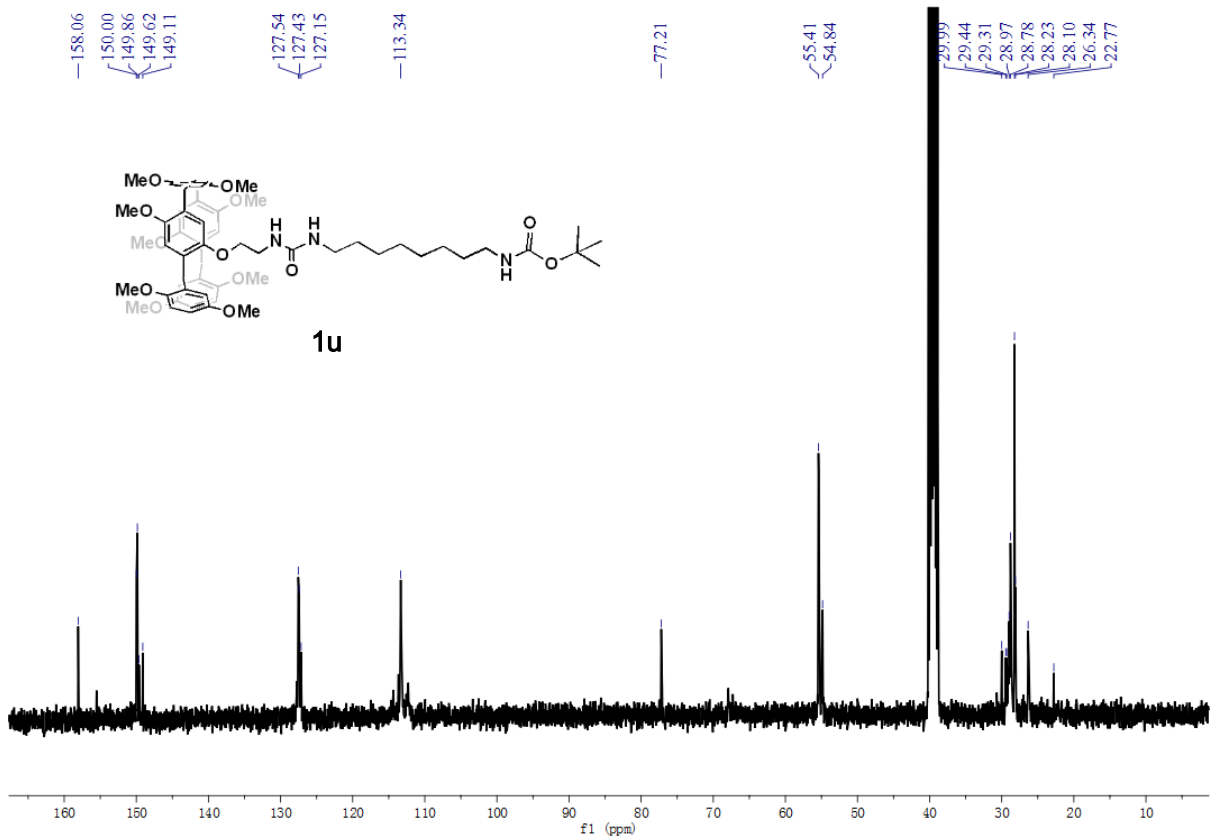

Figure S16. ^{13}C NMR spectrum (100 MHz, DMSO-d_6, 298 K) of compound **1u.**

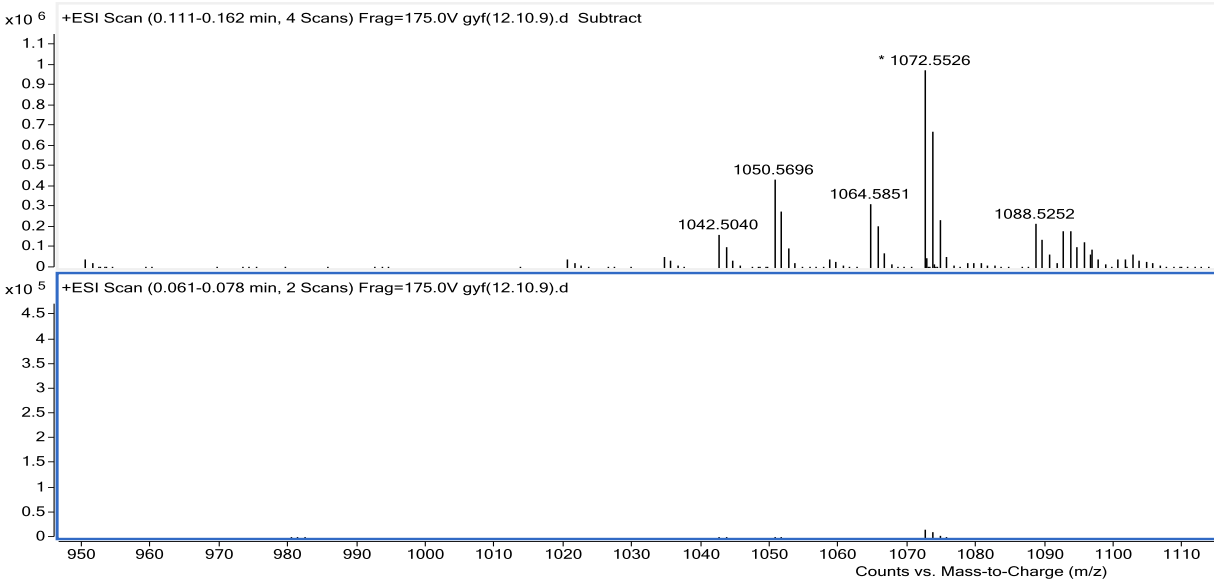

Figure S17. High resolution electrospray ionization mass spectrum of **1u**.

10.2 Compound **2** and **2u**

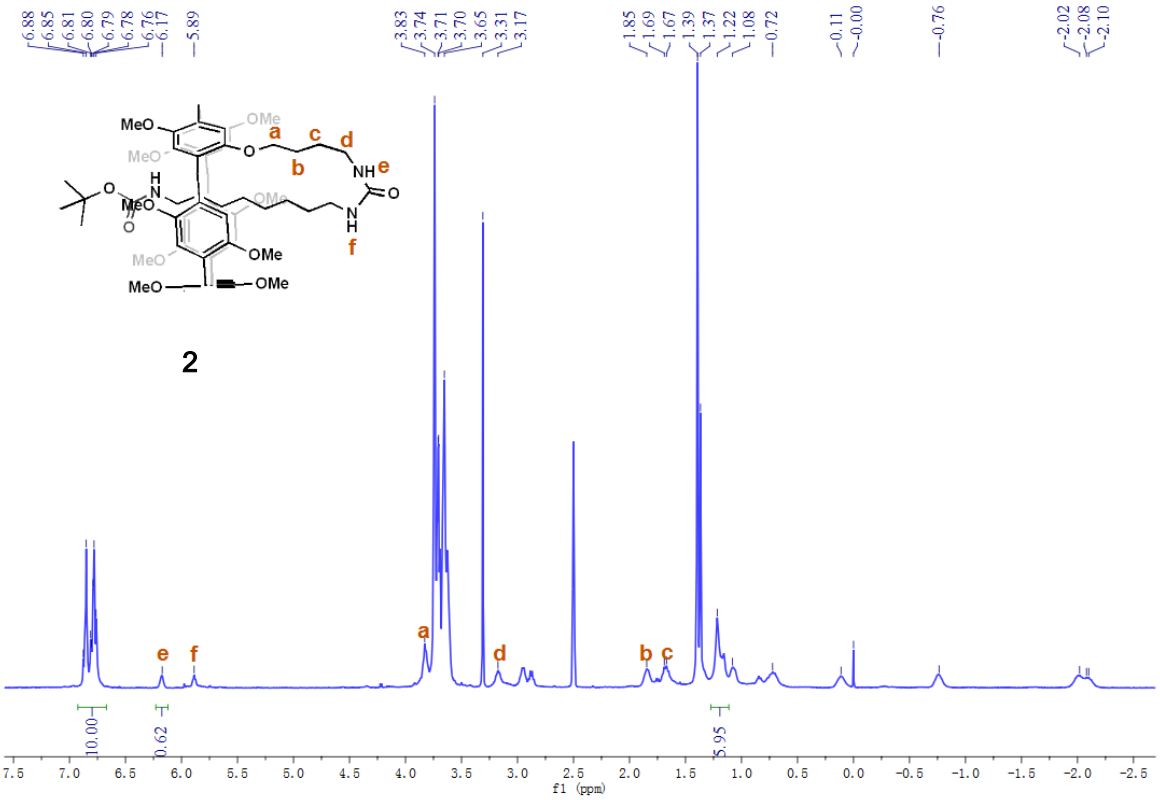

Figure S18. ^{1}H NMR spectrum (400 MHz, DMSO-d_6, 298 K) of compound **2.**

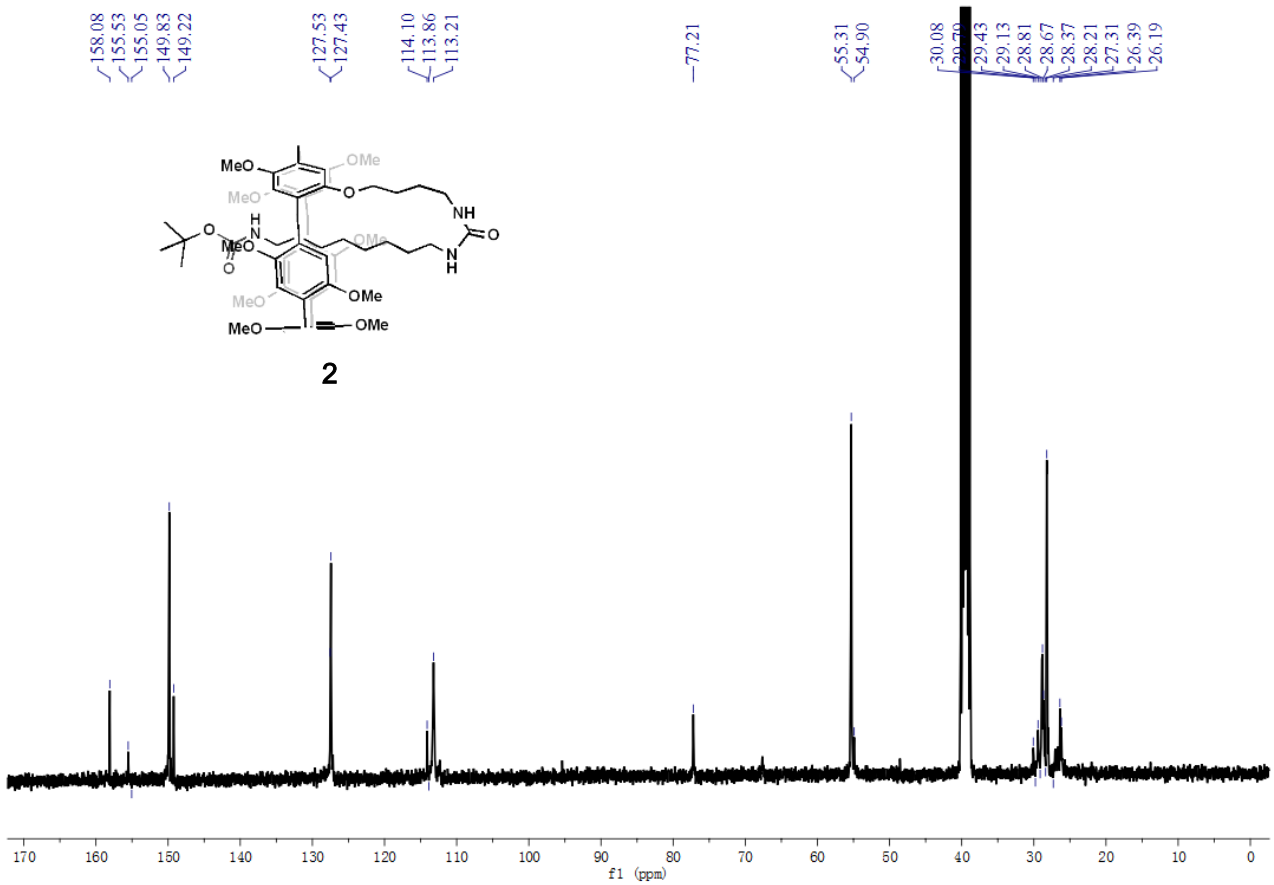

Figure S19. ^{13}C NMR spectrum (100 MHz, DMSO-d_6, 298 K) of compound **2.**

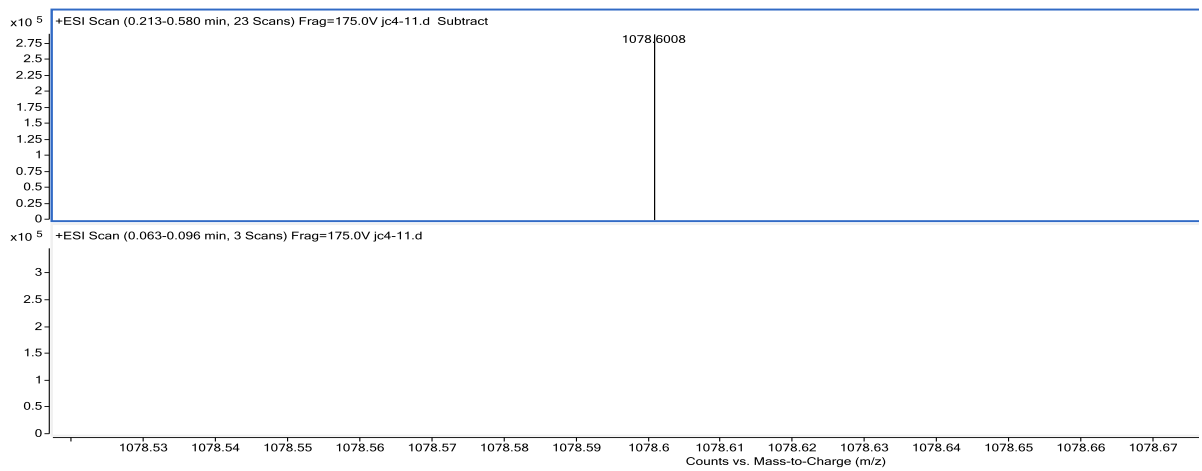

Figure S20. High resolution electrospray ionization mass spectrum of **2.**

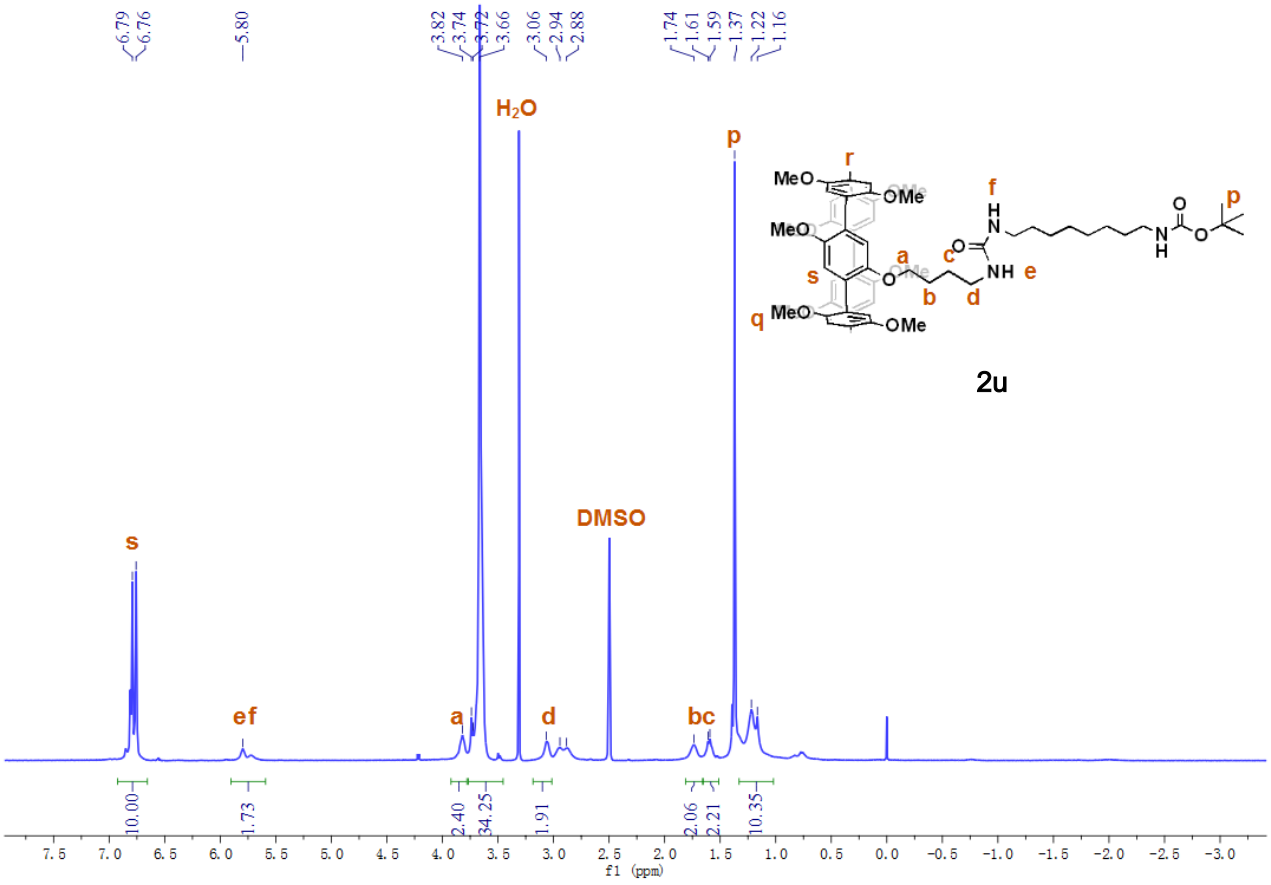

Figure S21. ^{1}H NMR spectrum (400 MHz, DMSO-d_6, 298 K) of compound **2u.**

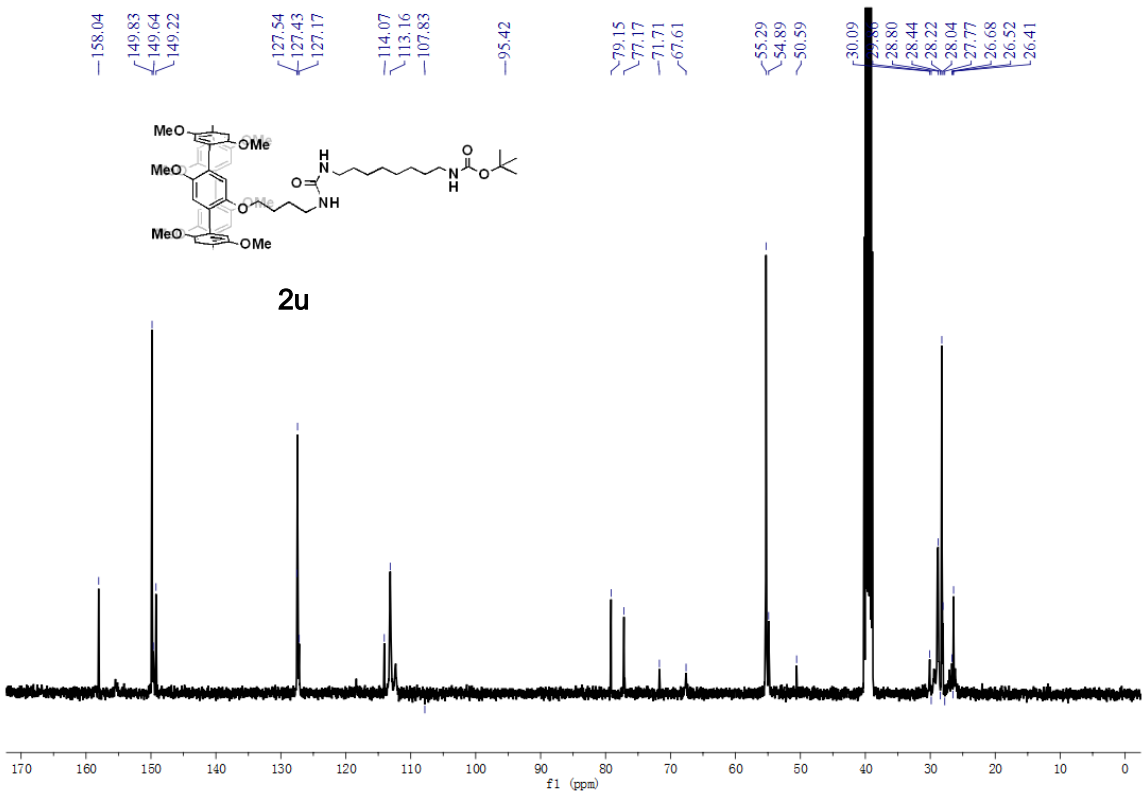

Figure S22. ^{13}C NMR spectrum (100 MHz, DMSO-d_6, 298 K) of compound **2u.**

10.3 Compound **3**

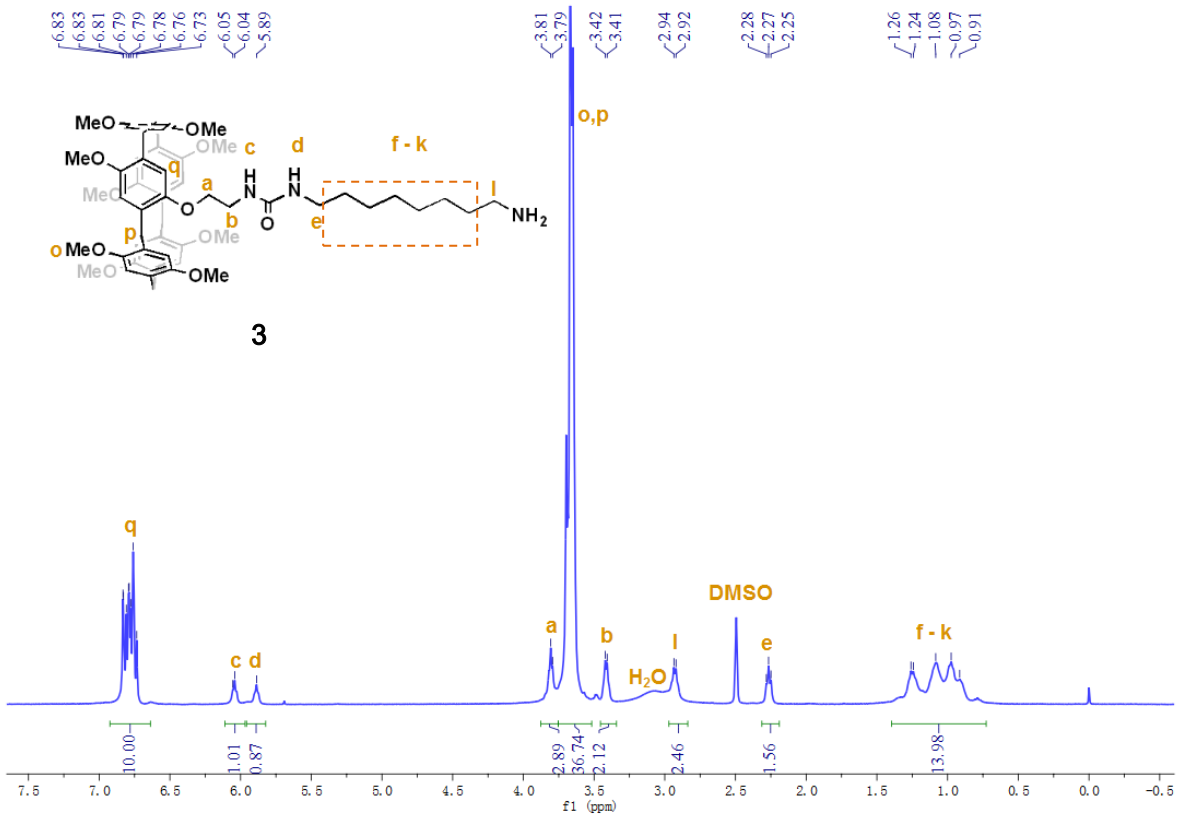

Figure S23. ^{1}H NMR spectrum (400 MHz, DMSO-d_6, 298 K) of compound **3.**

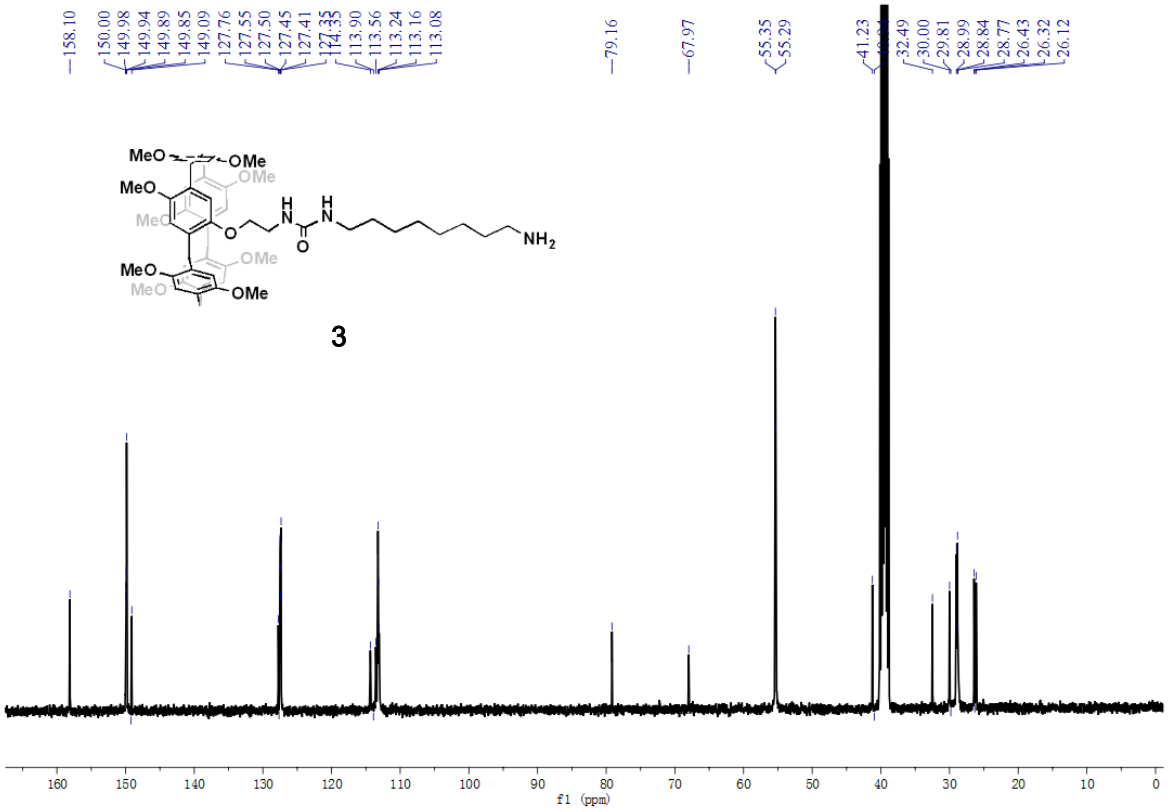

Figure S24. ^{13}C NMR spectrum (100 MHz, DMSO-d_6, 298 K) of compound **3.**

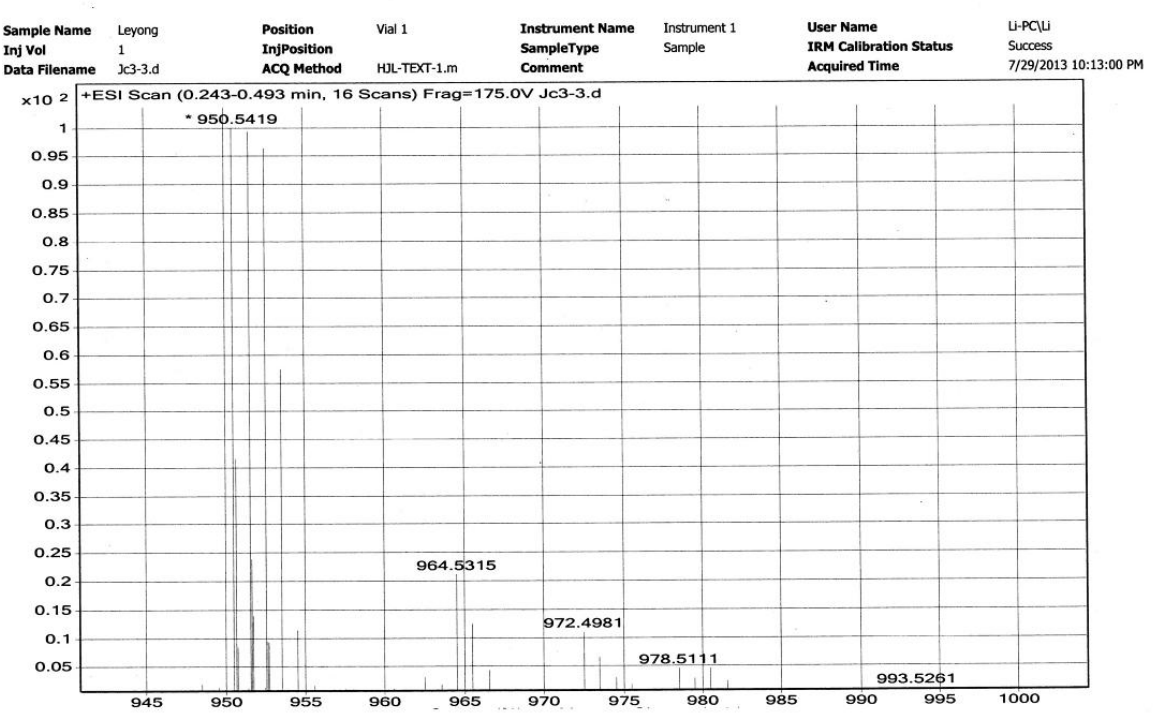

Figure S25. High resolution electrospray ionization mass spectrum of **3** (CH3CN).

10.4 Compound **4**

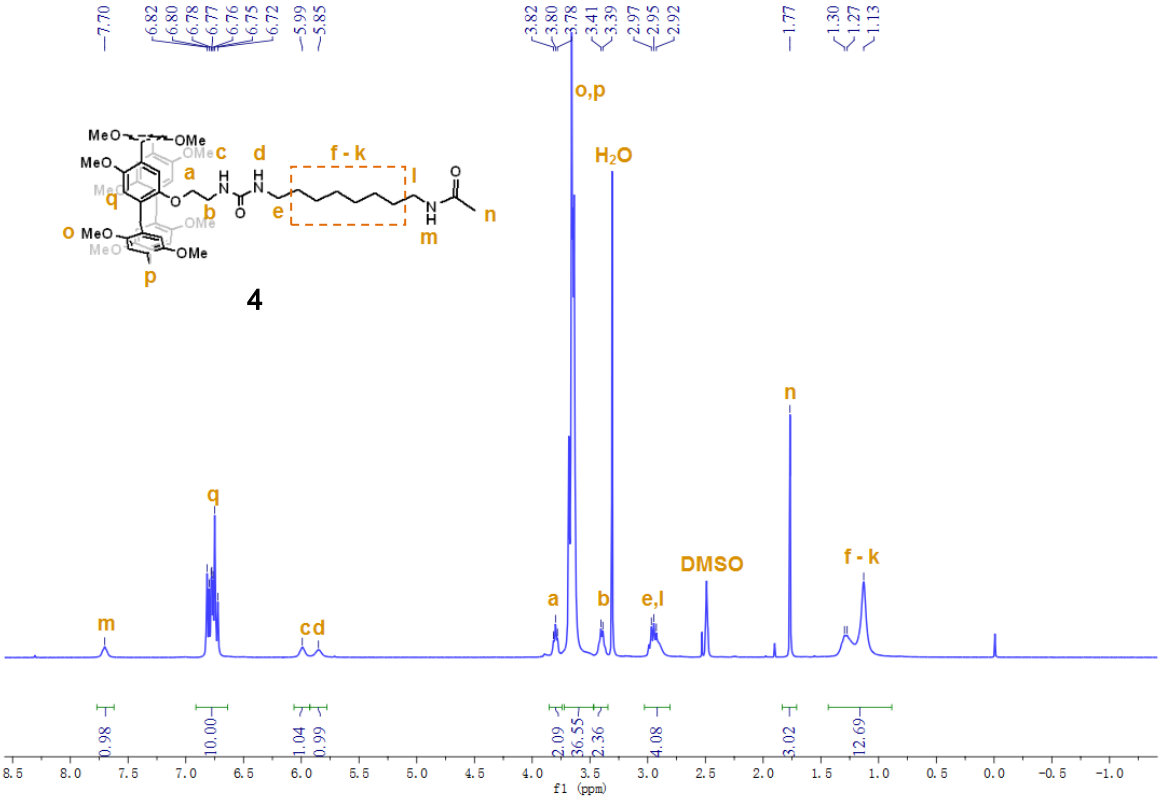

Figure S26. ^{1}H NMR spectrum (400 MHz, DMSO-d_6, 298 K) of compound **4.**

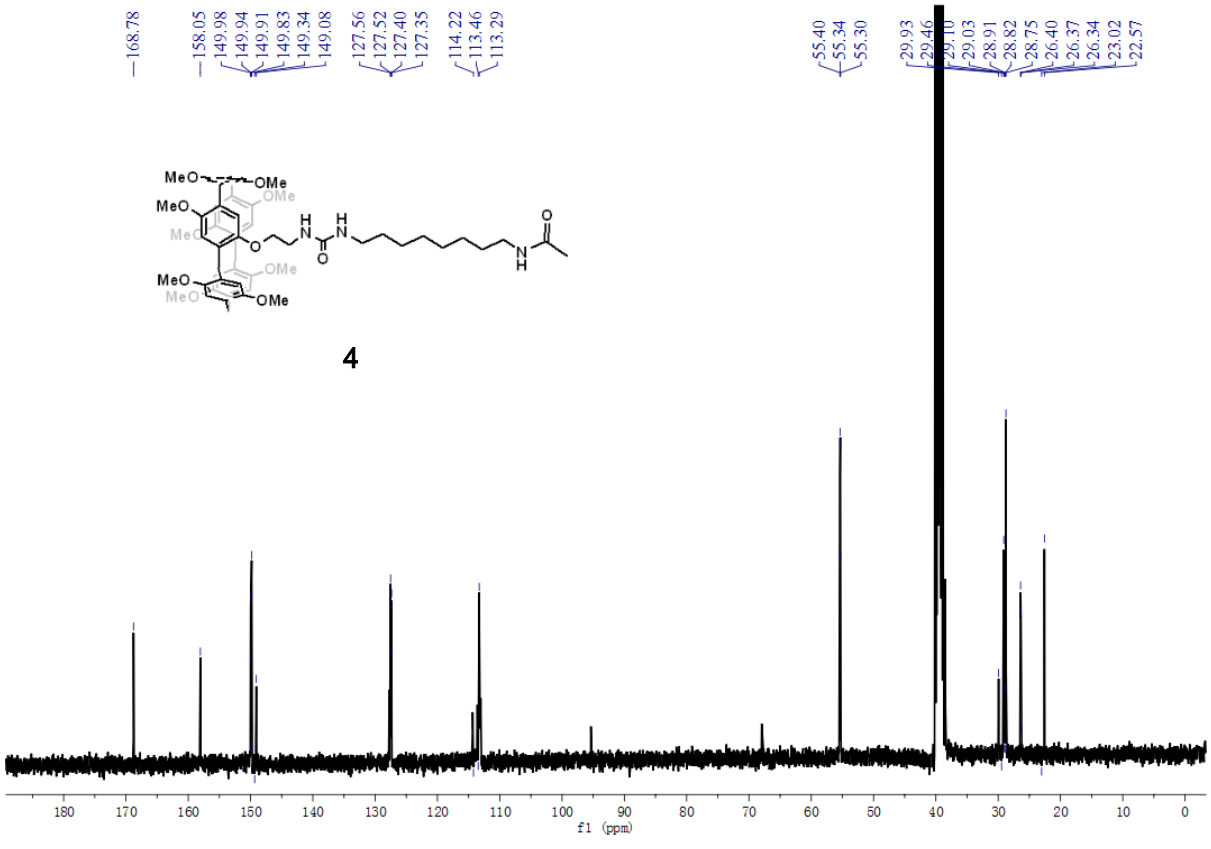

Figure S27. ^{13}C NMR spectrum (100 MHz, DMSO-d_6, 298 K) of compound **4.**

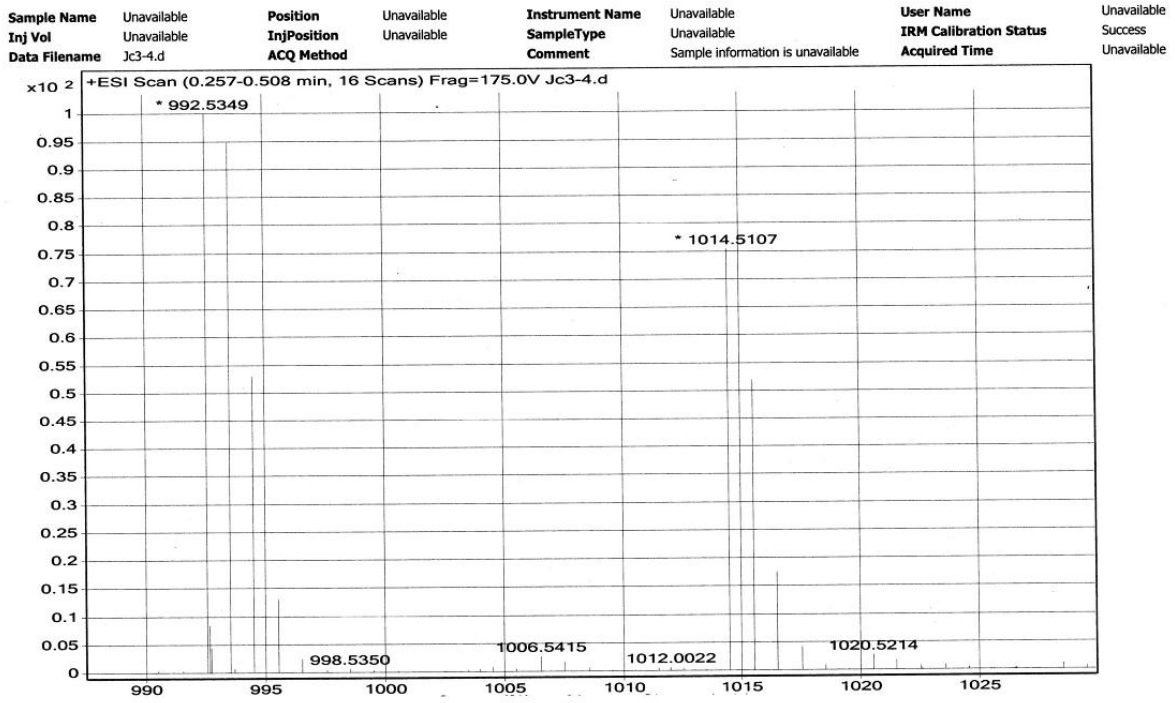

Figure S28. High resolution electrospray ionization mass spectrum of **4** (CH3CN).

10.5 Compound **5**

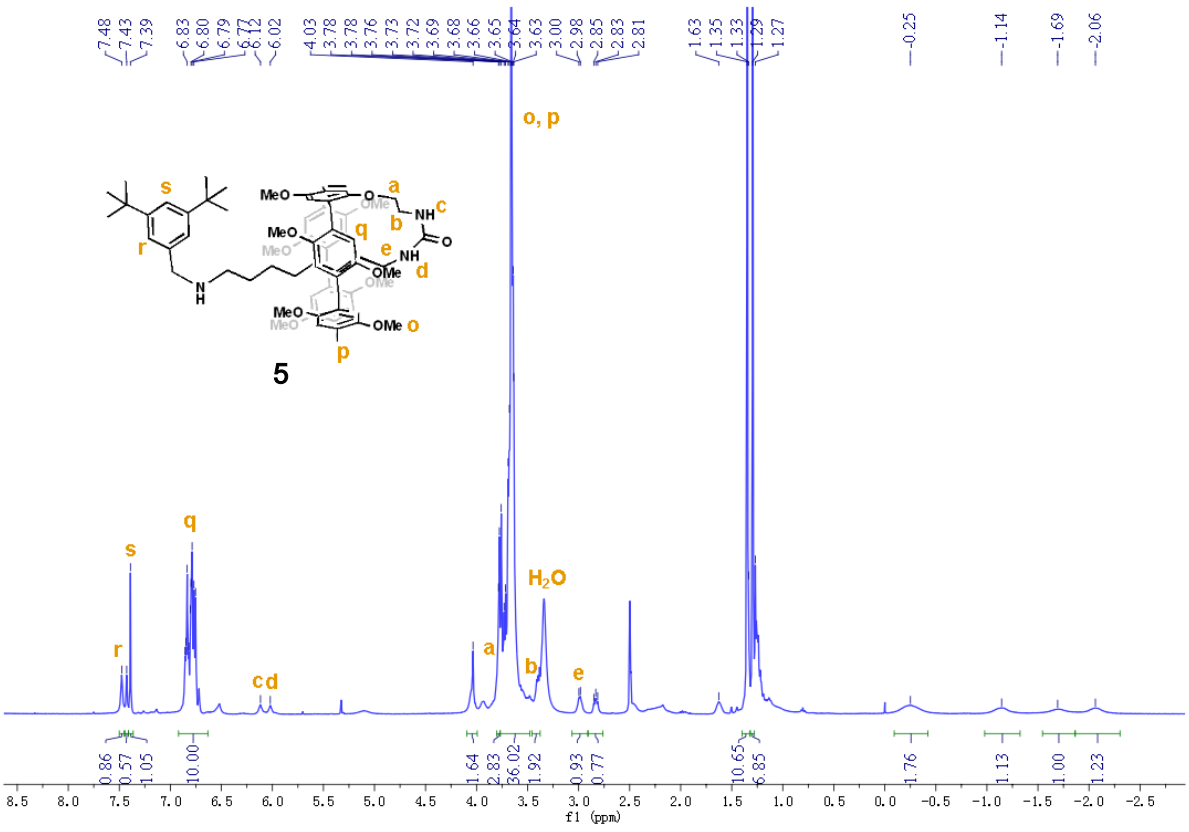

Figure S29. ^{1}H NMR spectrum (400 MHz, DMSO-d_6, 298 K) of compound **5.**

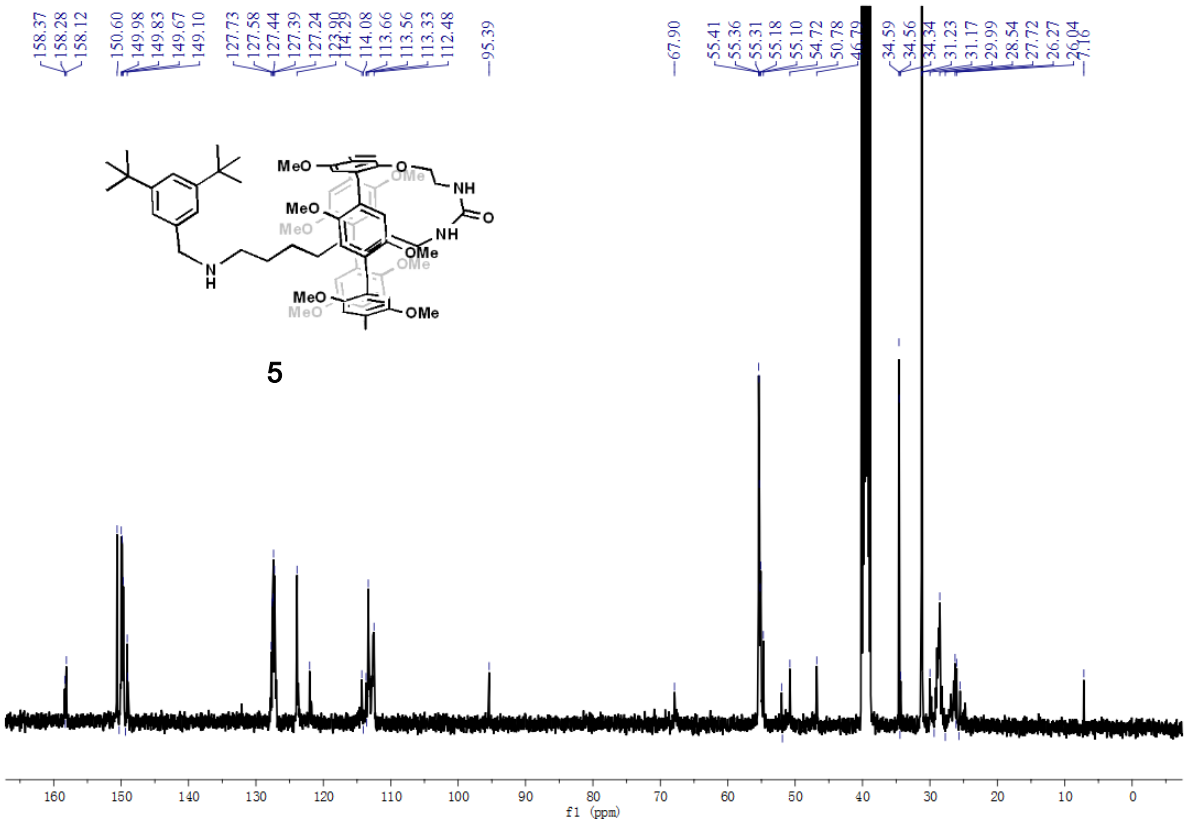

Figure S30. ^{13}C NMR spectrum (100 MHz, DMSO-d_6, 298 K) of compound **5.**

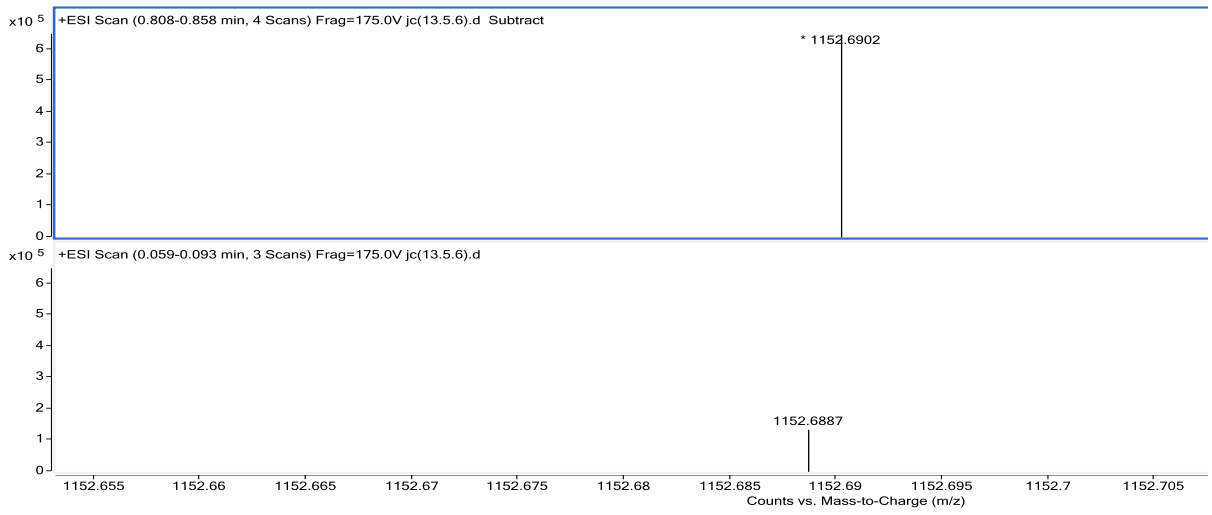

Figure S31. High resolution electrospray ionization mass spectrum of **5** (CH_3CN).

10.6 Compound **6**

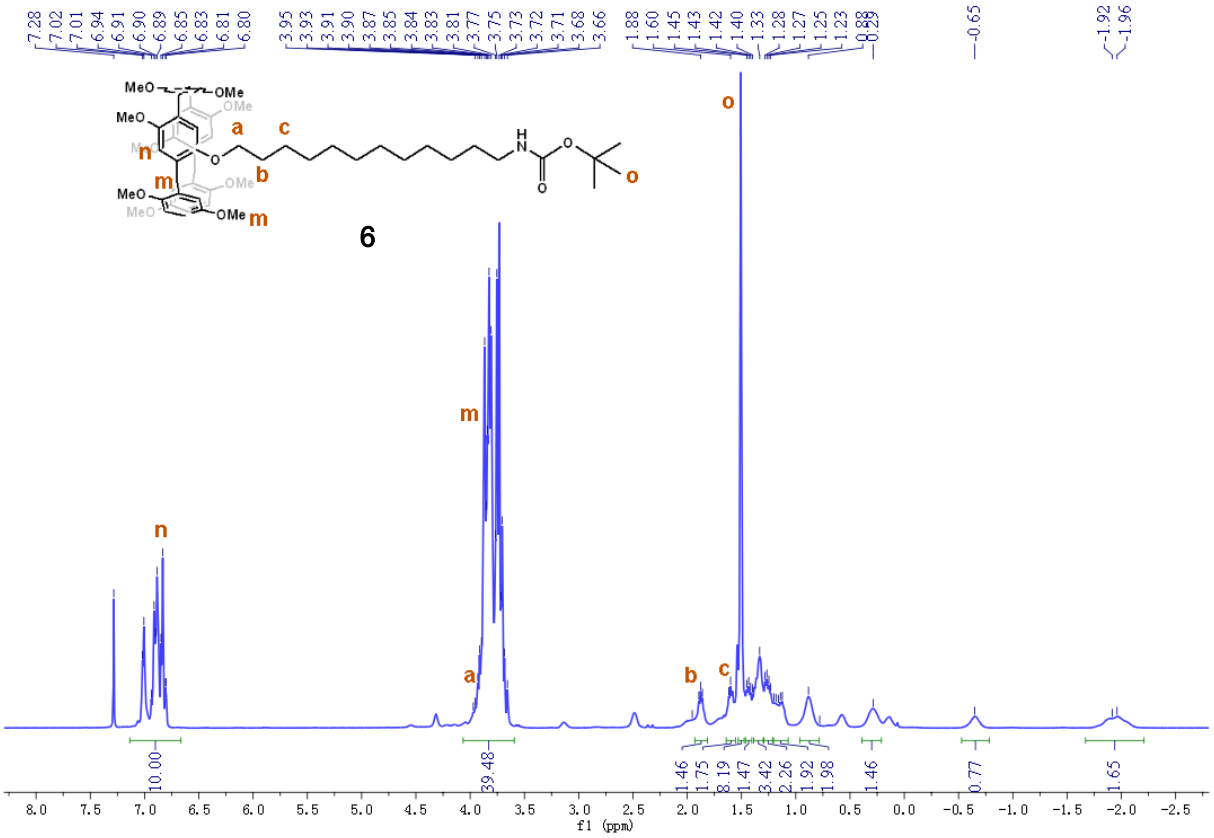

Figure S32. ^{1}H NMR spectrum (400 MHz, $CDCl_3$, 298 K) of compound **6.**

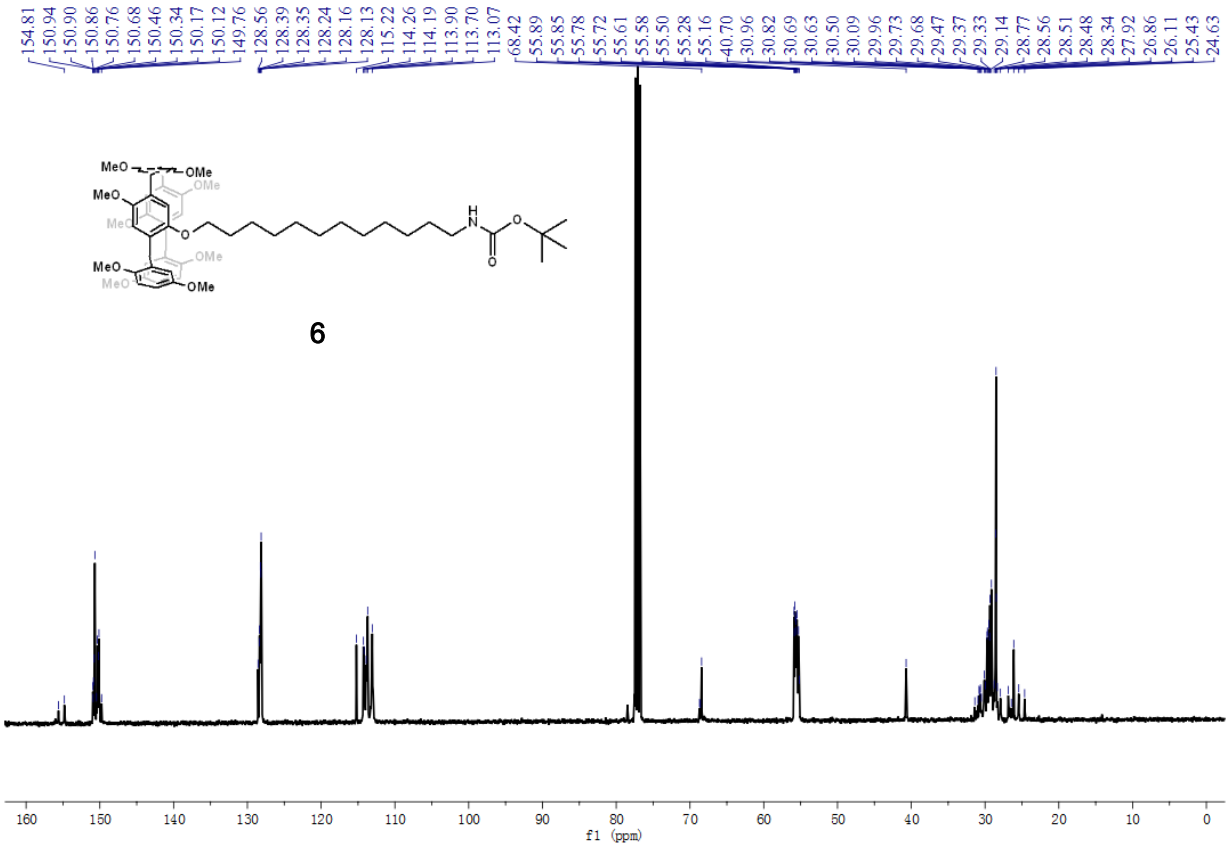

Figure S33. ^{13}C NMR spectrum (100 MHz, $CDCl_3$, 298 K) of compound **6.**

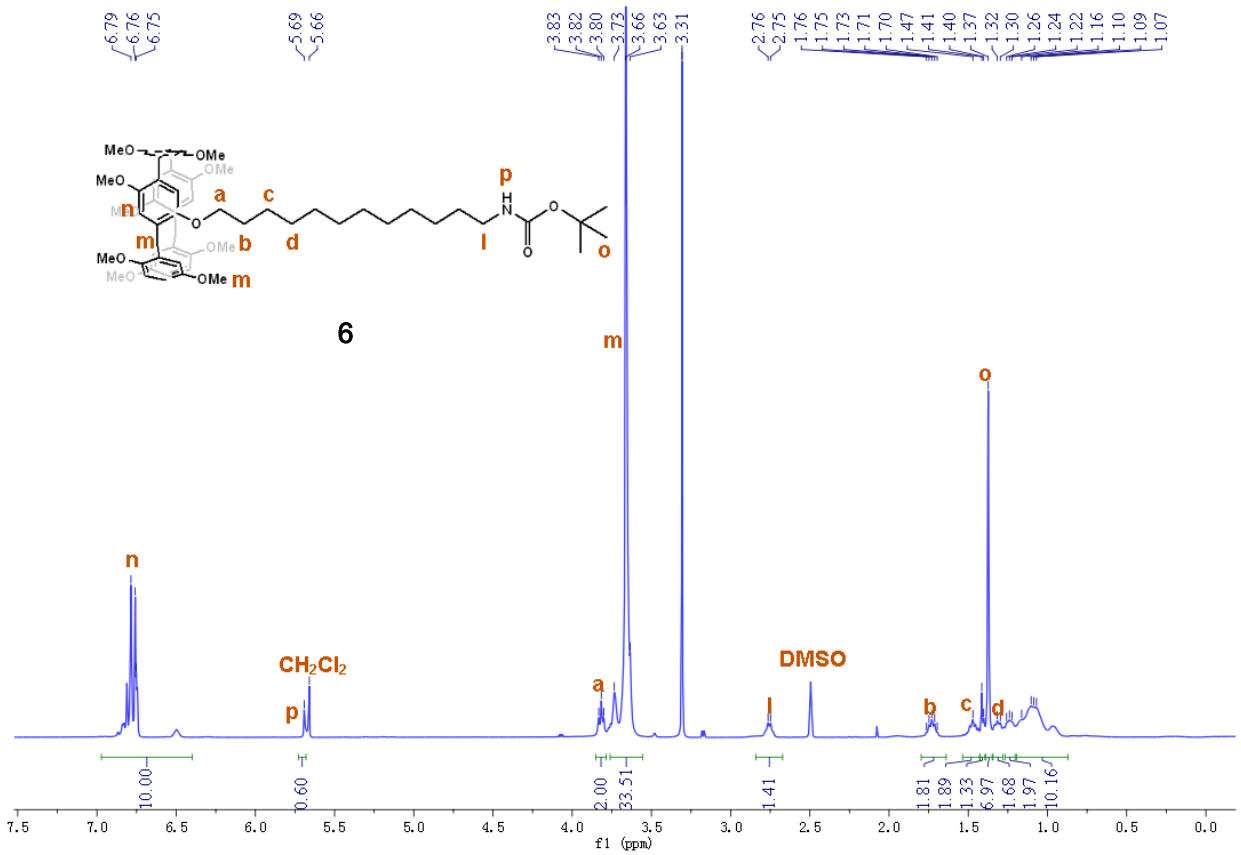

Figure S34. ^{1}H NMR spectrum (400 MHz, DMSO-d_6, 298 K) of compound **6.**

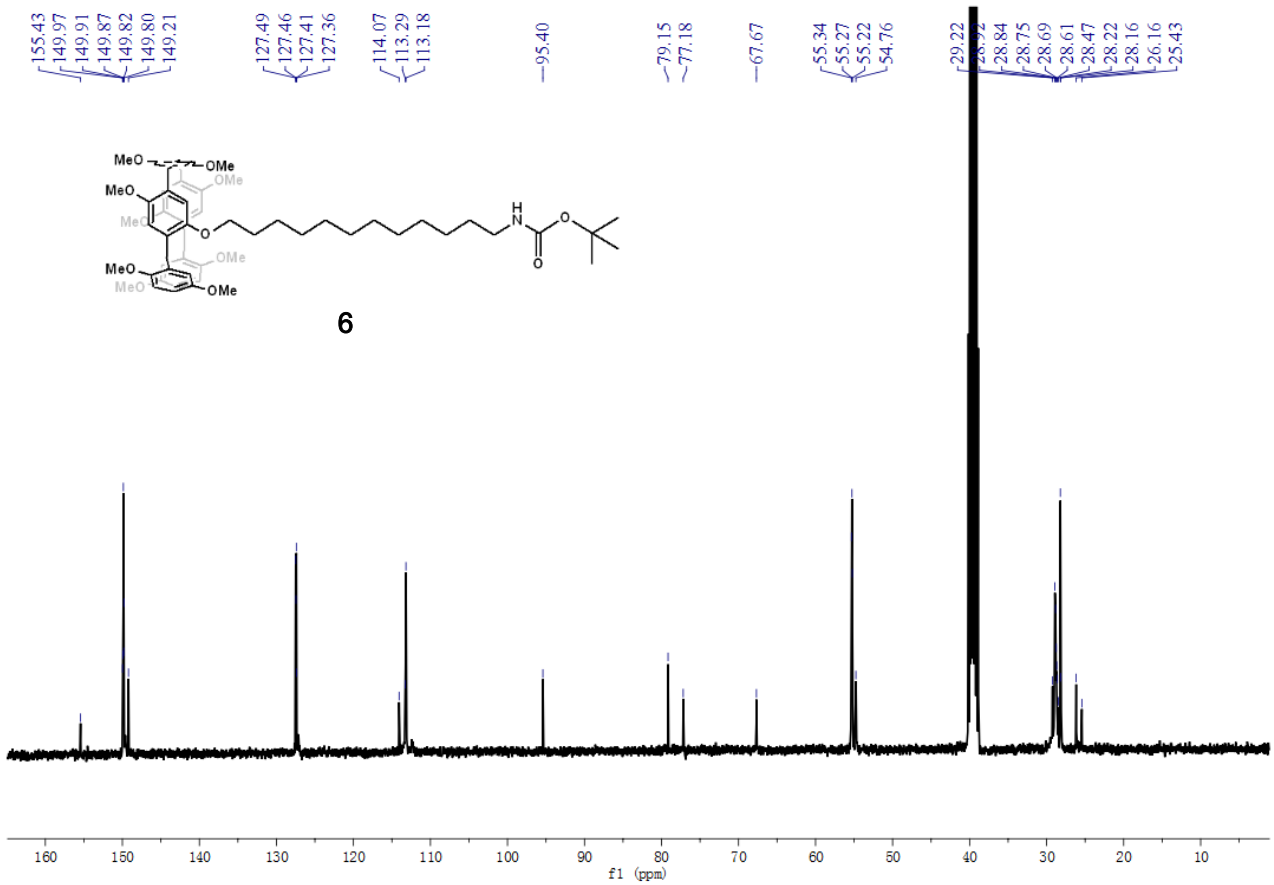

Figure S35. ^{13}C NMR spectrum (100 MHz, DMSO-d_6, 298 K) of compound **6.**

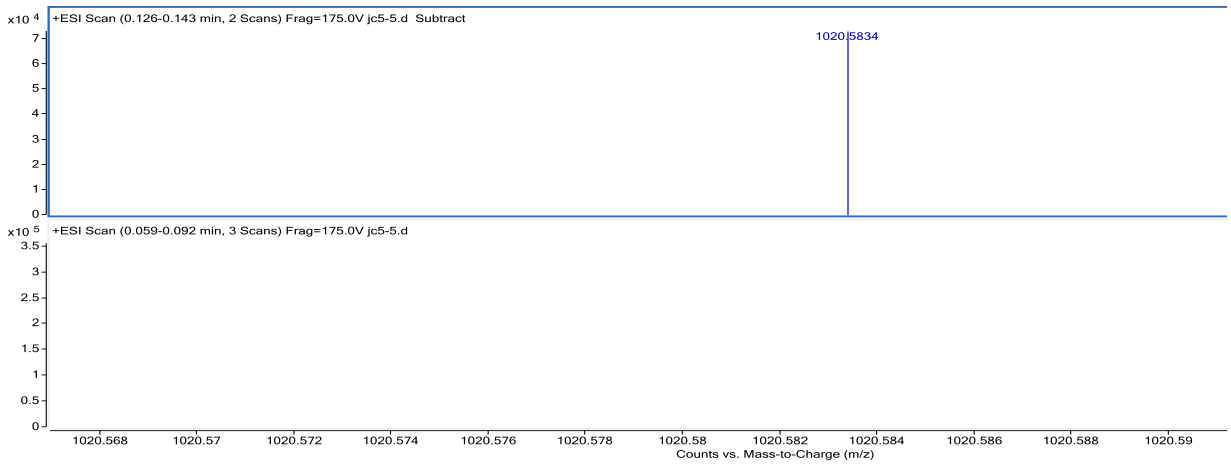

Figure S36. High resolution electrospray ionization mass spectrum of **6** (CH_3CN).

10.7 Compound **7u**

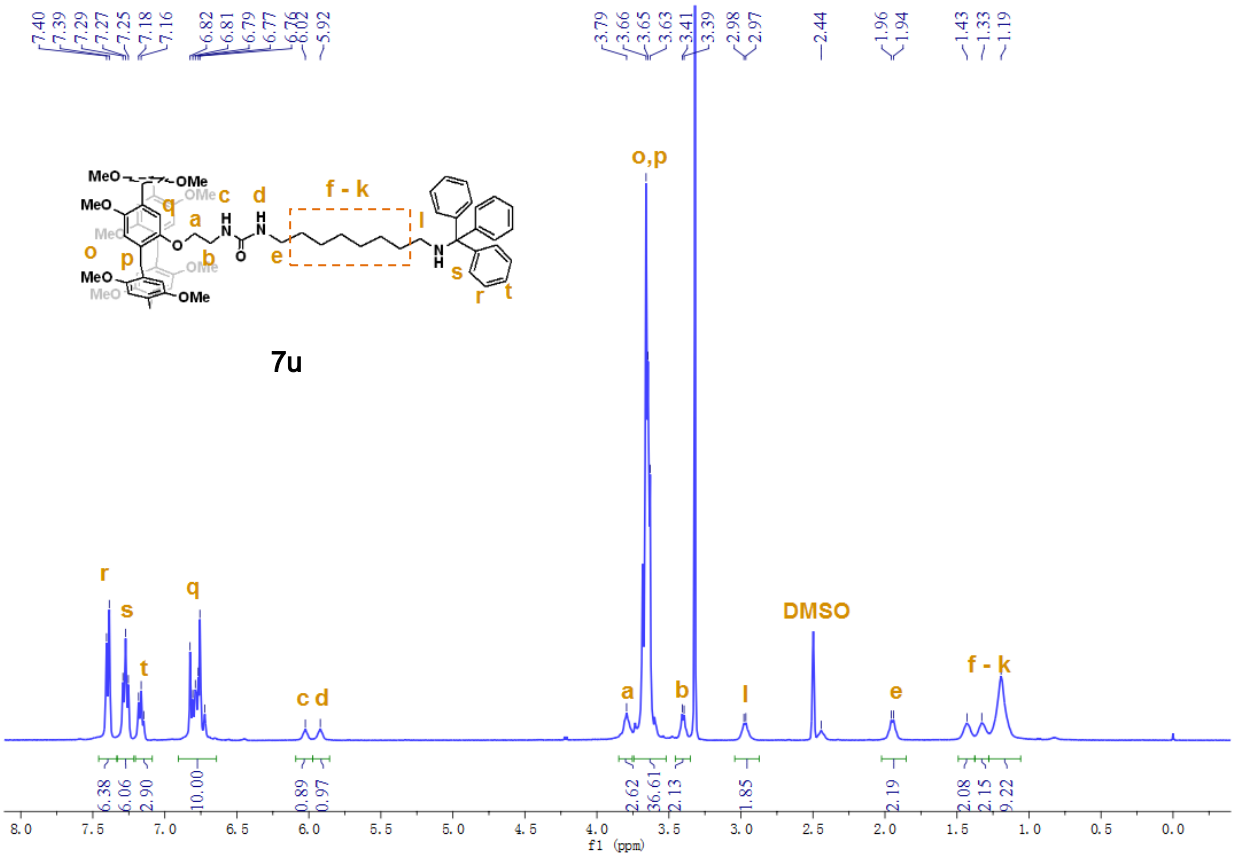

Figure S37. ^{1}H NMR spectrum (400 MHz, DMSO-d_6, 298 K) of compound **7u.**

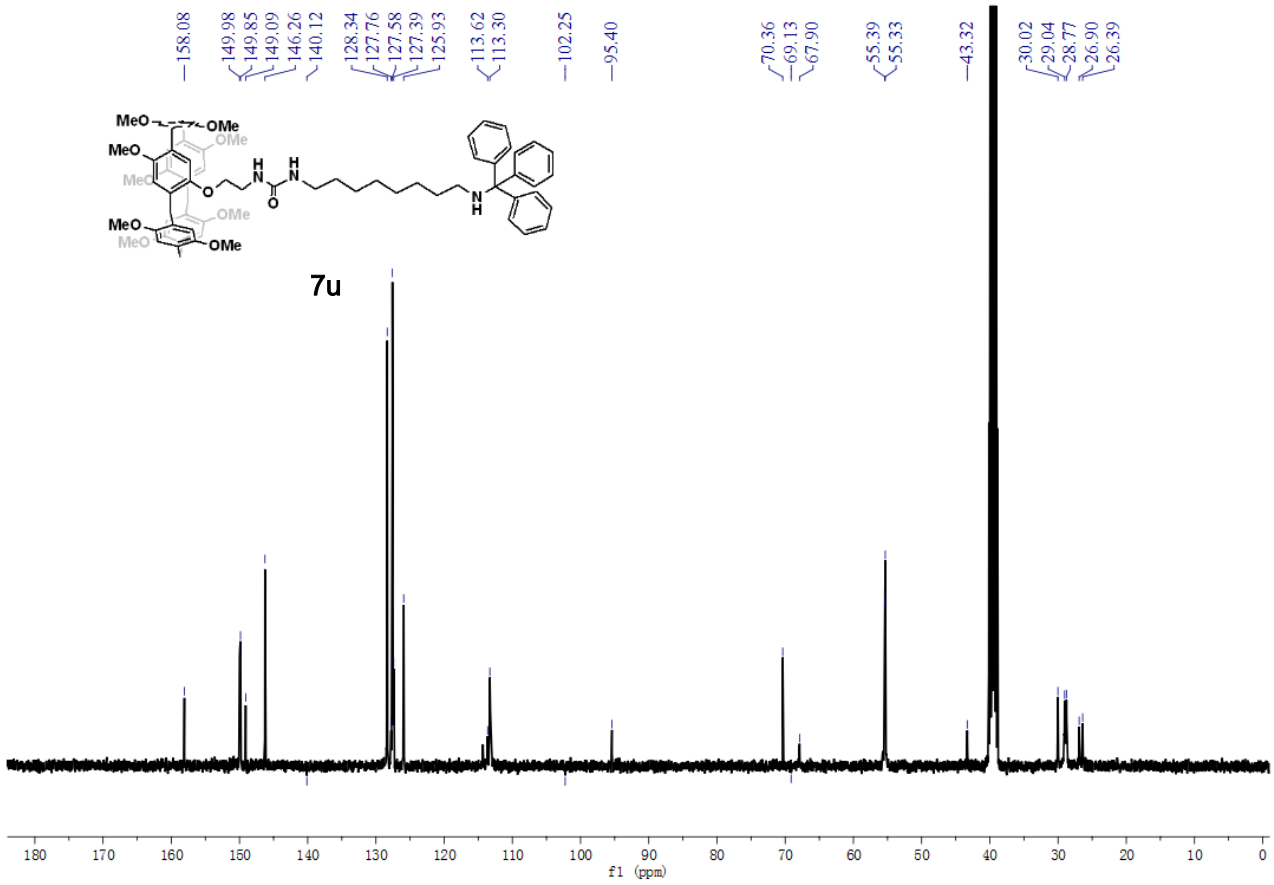

Figure S38. ^{13}C NMR spectrum (100 MHz, DMSO-d_6, 298 K) of compound **7u.**

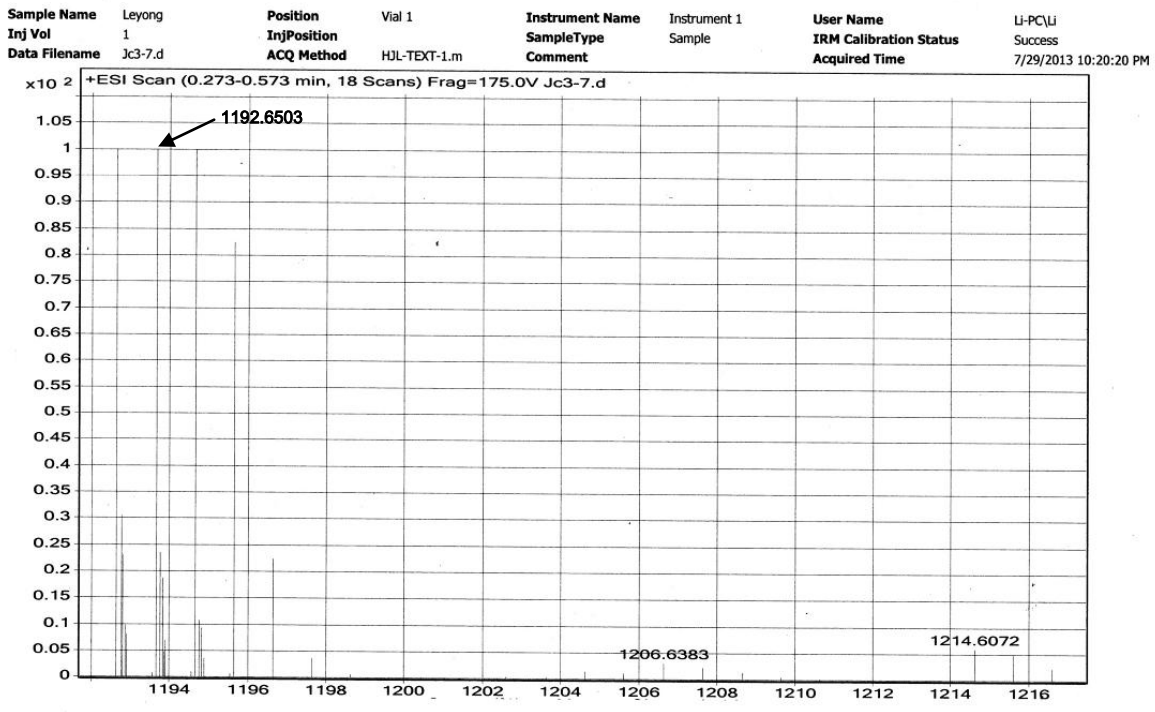

Figure S39. High resolution electrospray ionization mass spectrum of **7u** (CH3CN).

10.8 Compound **9**

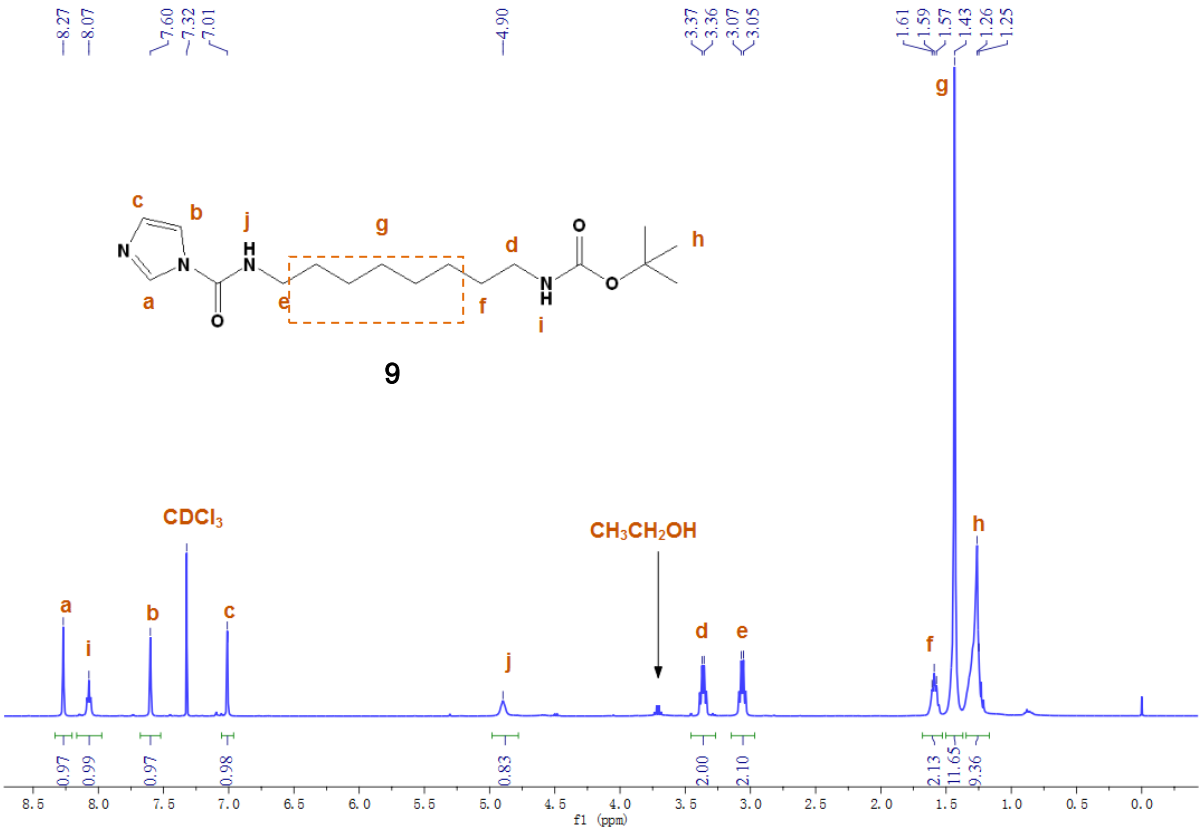

Figure S40. ^{1}H NMR spectrum (300 MHz, $CDCl_3$, 298 K) of compound **9.**

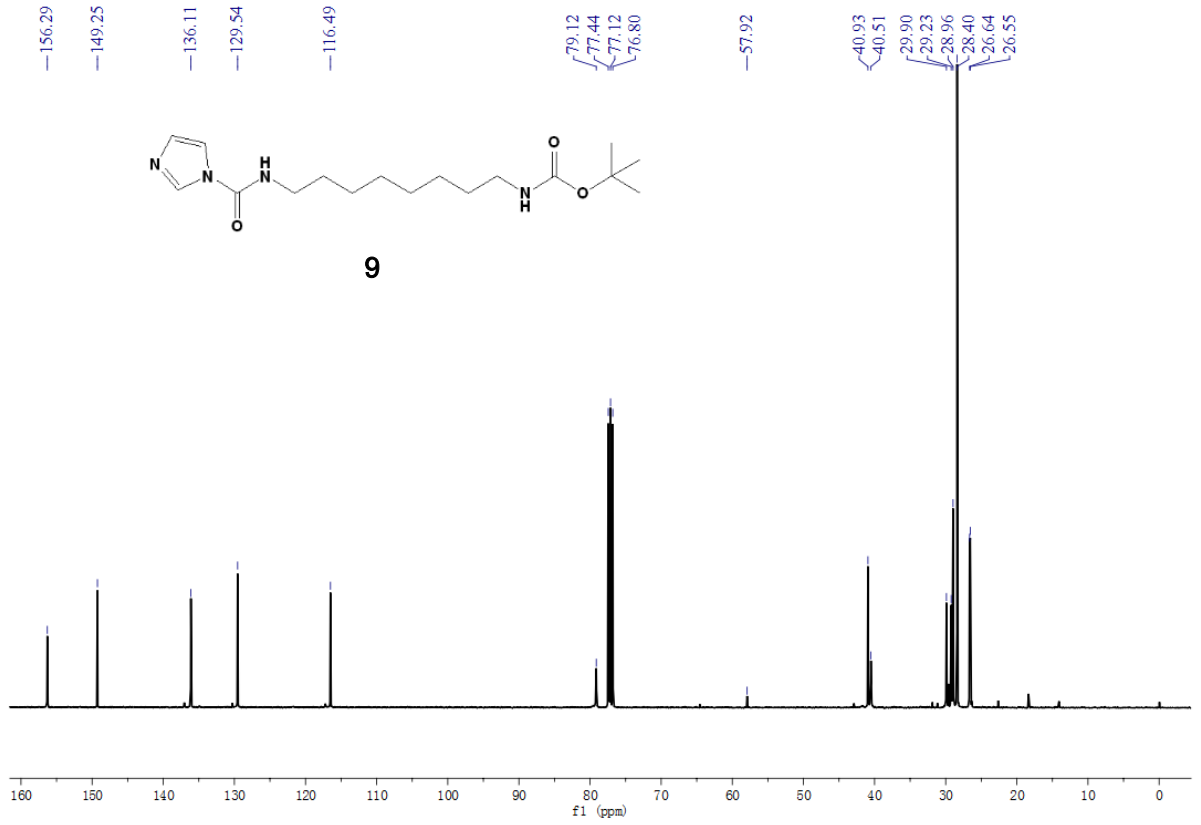

Figure S41. ^{1}H NMR spectrum (100 MHz, $CDCl_3$, 298 K) of compound **9.**

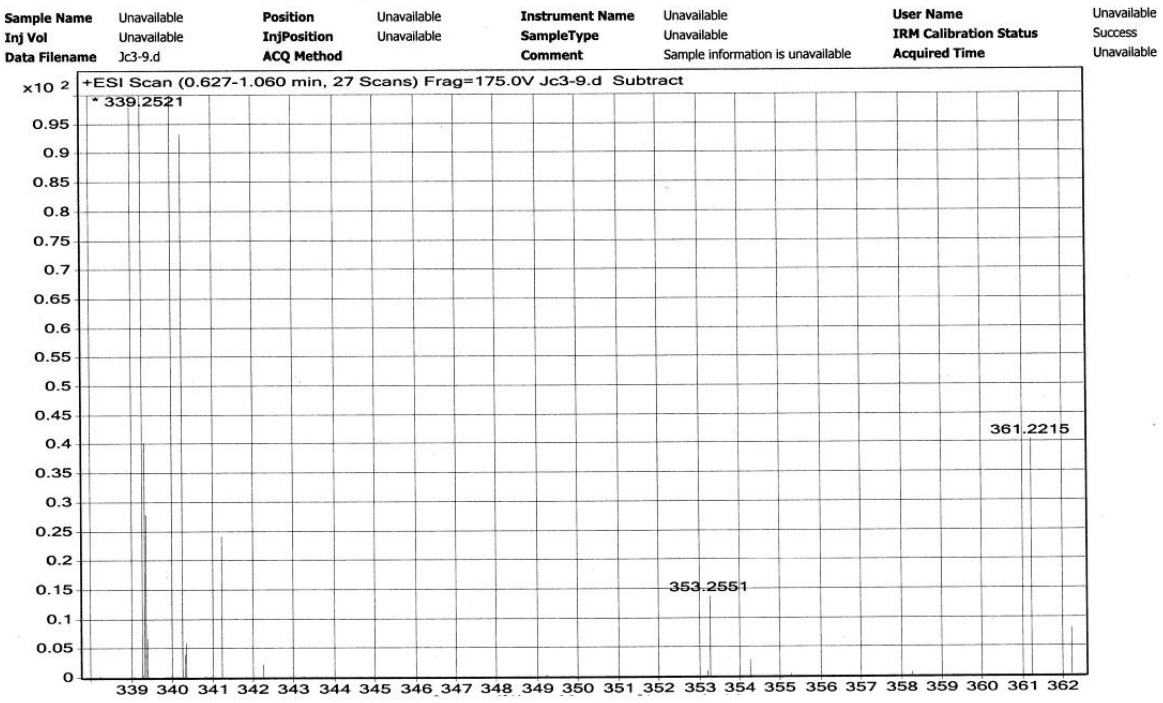

Figure S42. High resolution electrospray ionization mass spectrum of **9** (CH_3OH).

10.9 Compound **10**

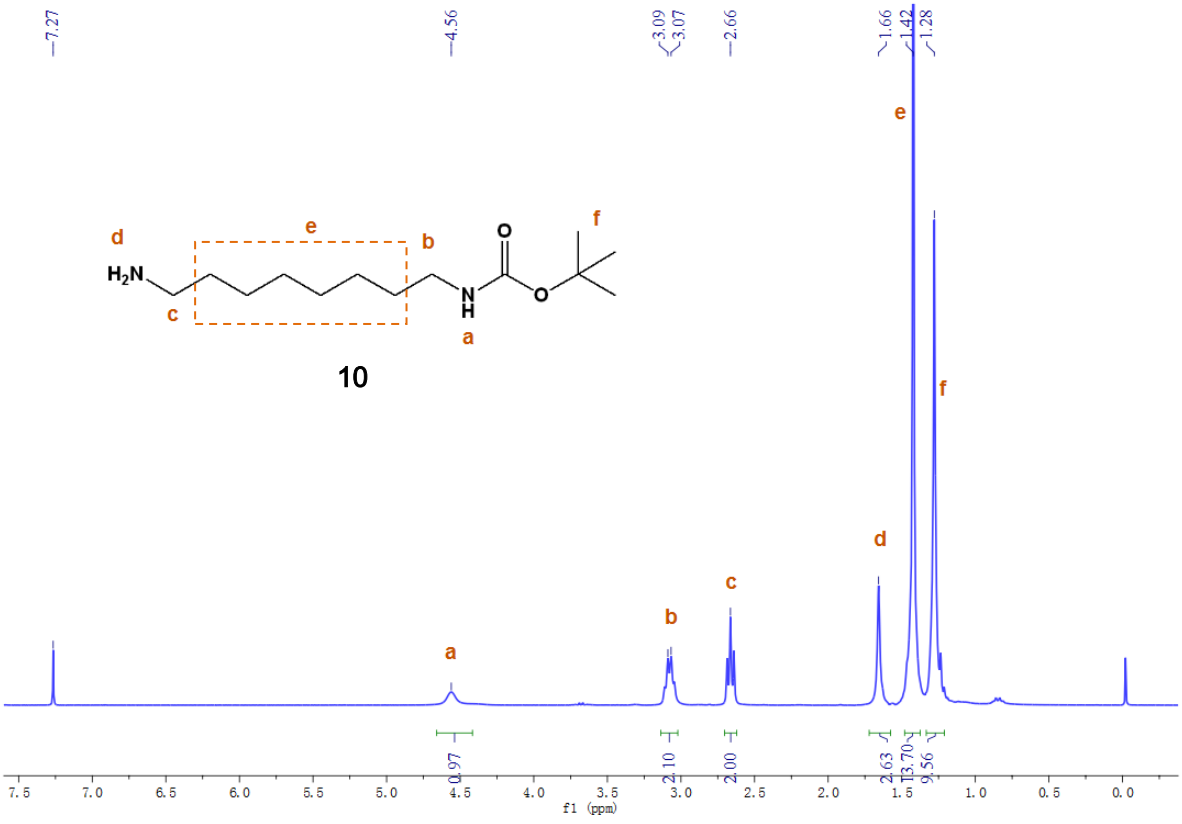

Figure S43. ^{1}H NMR spectrum (400 MHz, $CDCl_3$, 298 K) of compound **10.**

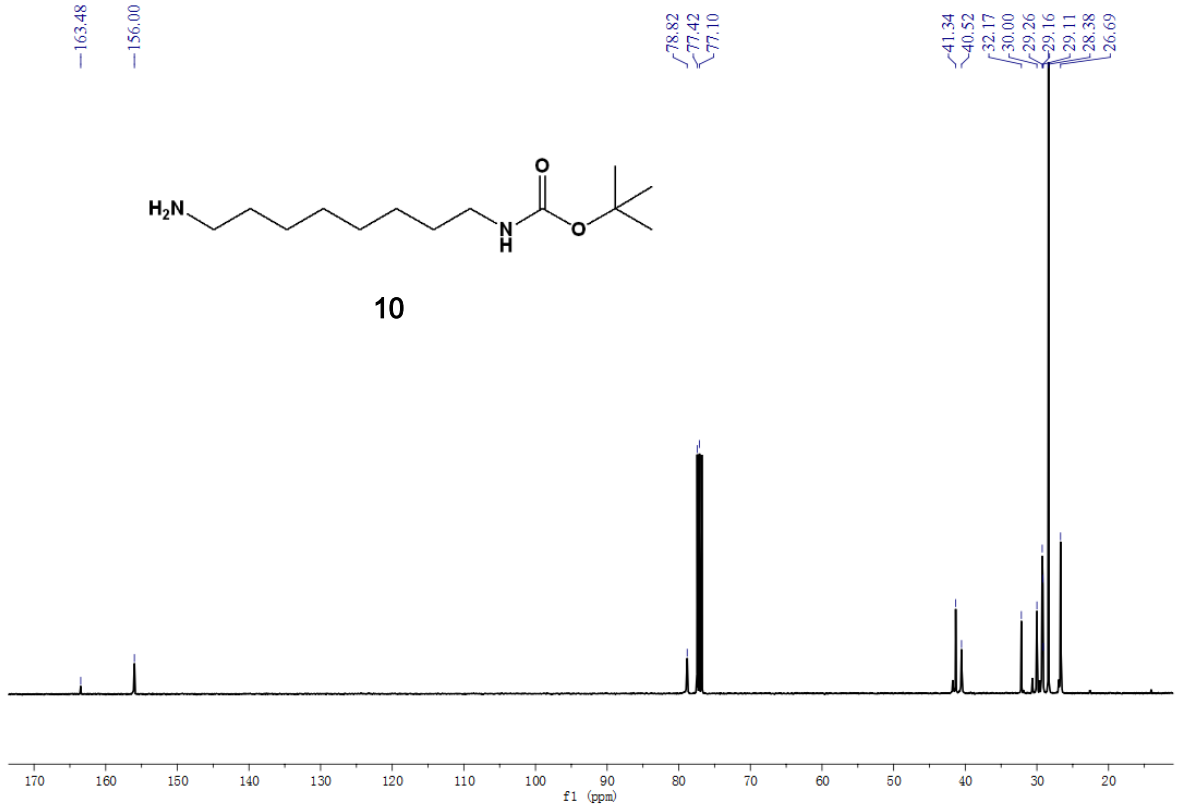

Figure S44. ^{13}C NMR spectrum (100 MHz, $CDCl_3$, 298 K) of compound **10.**

10.10 Compound **11**

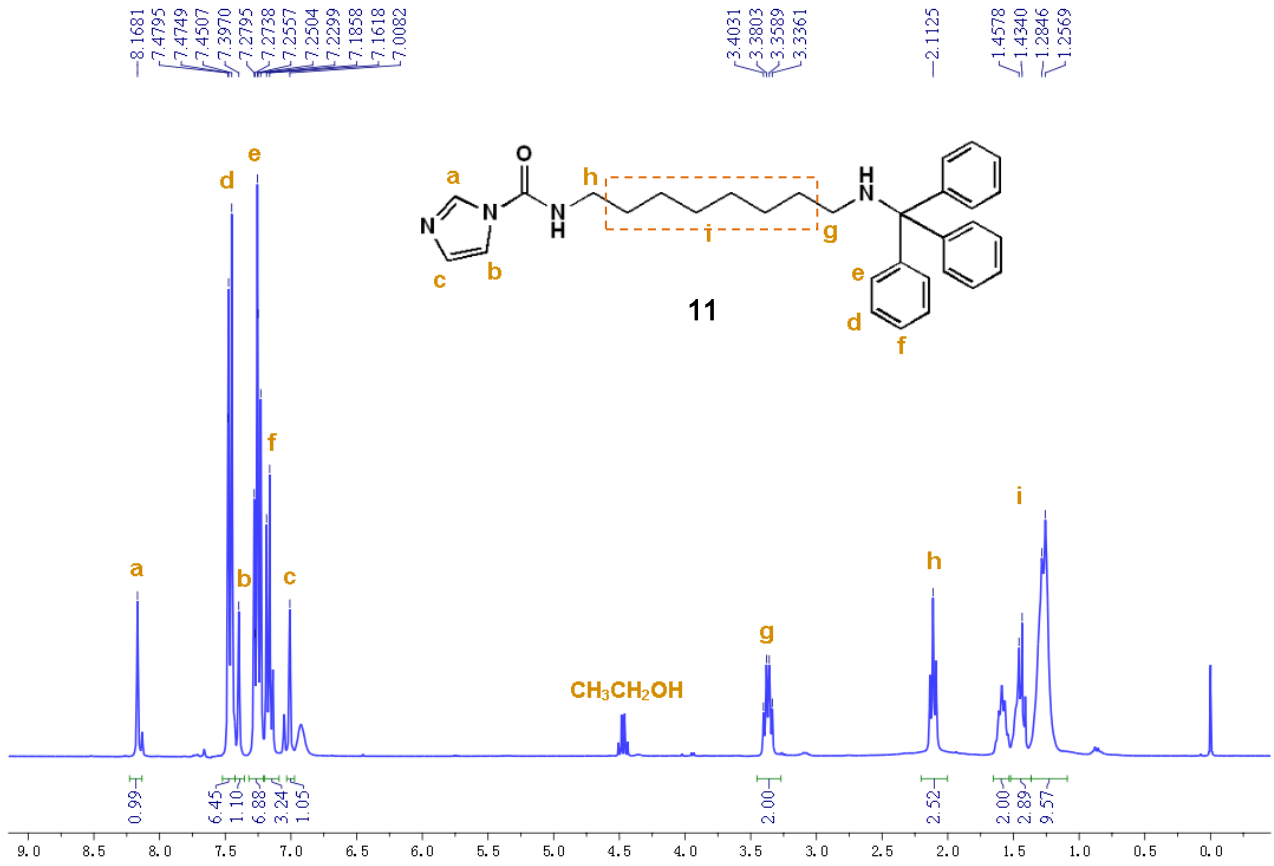

Figure S45. ^{1}H NMR spectrum (300 MHz, $CDCl_3$, 298 K) of compound **11.**

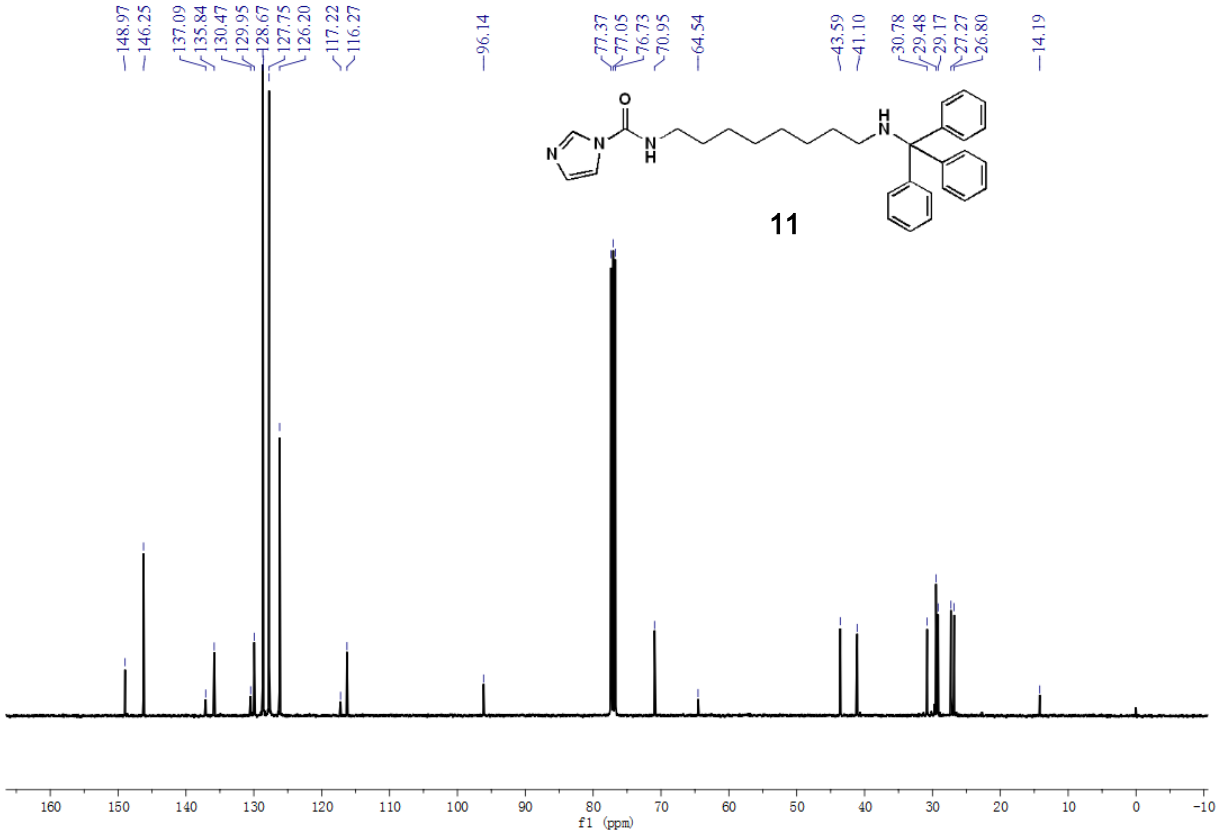

Figure S46. ^{13}C NMR spectrum (100 MHz, $CDCl_3$, 298 K) of compound **11.**

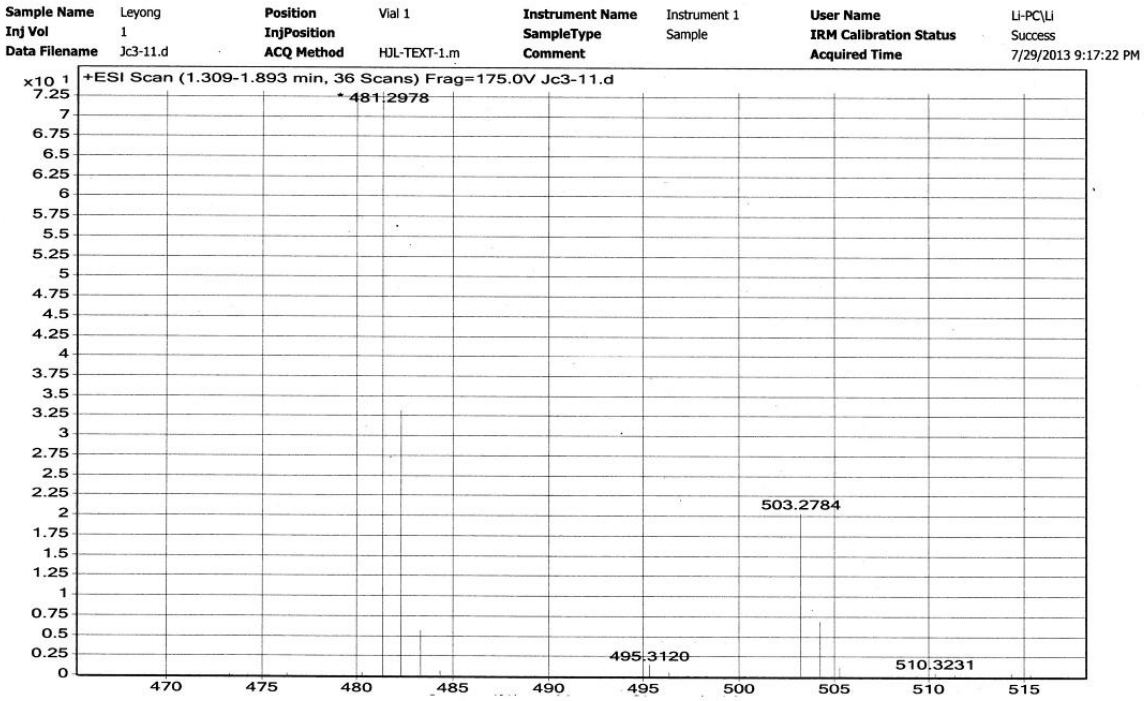

Figure S47. High resolution electrospray ionization mass spectrum of **11** (CH_3OH).

10.11 Compound **12**

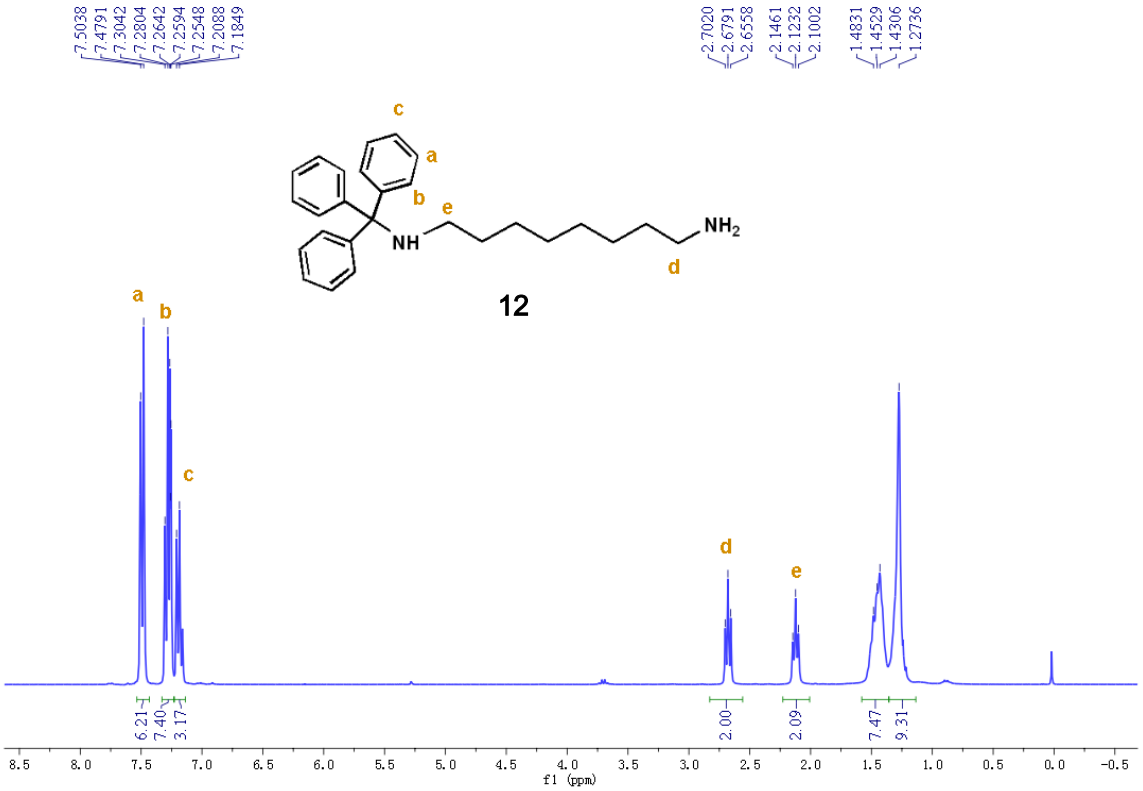

Figure S48. ^{1}H NMR spectrum (300 MHz, $CDCl_3$, 298 K) of compound **12.**

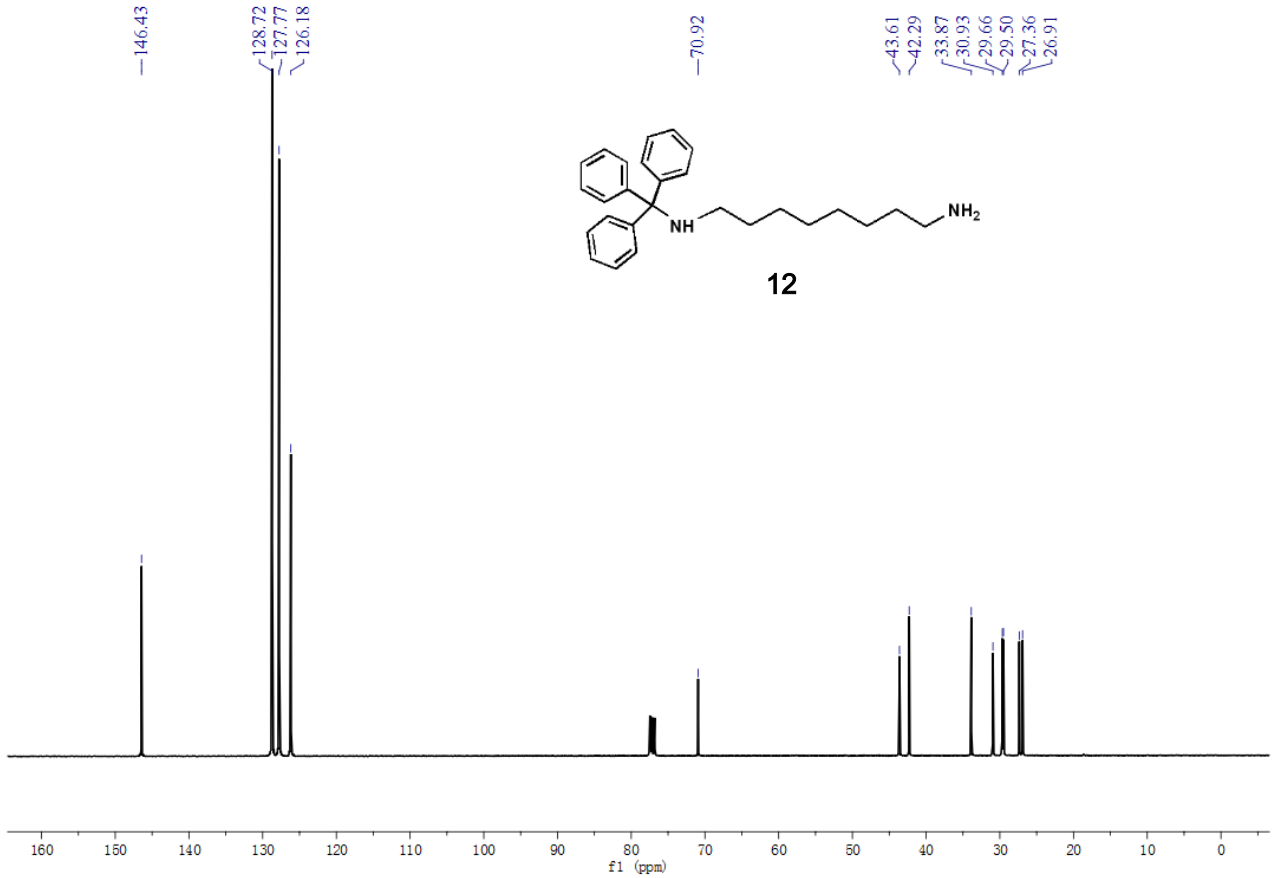

Figure S49. ^{13}C NMR spectrum (100 MHz, $CDCl_3$, 298 K) of compound **12.**

10.12 Compound **13**

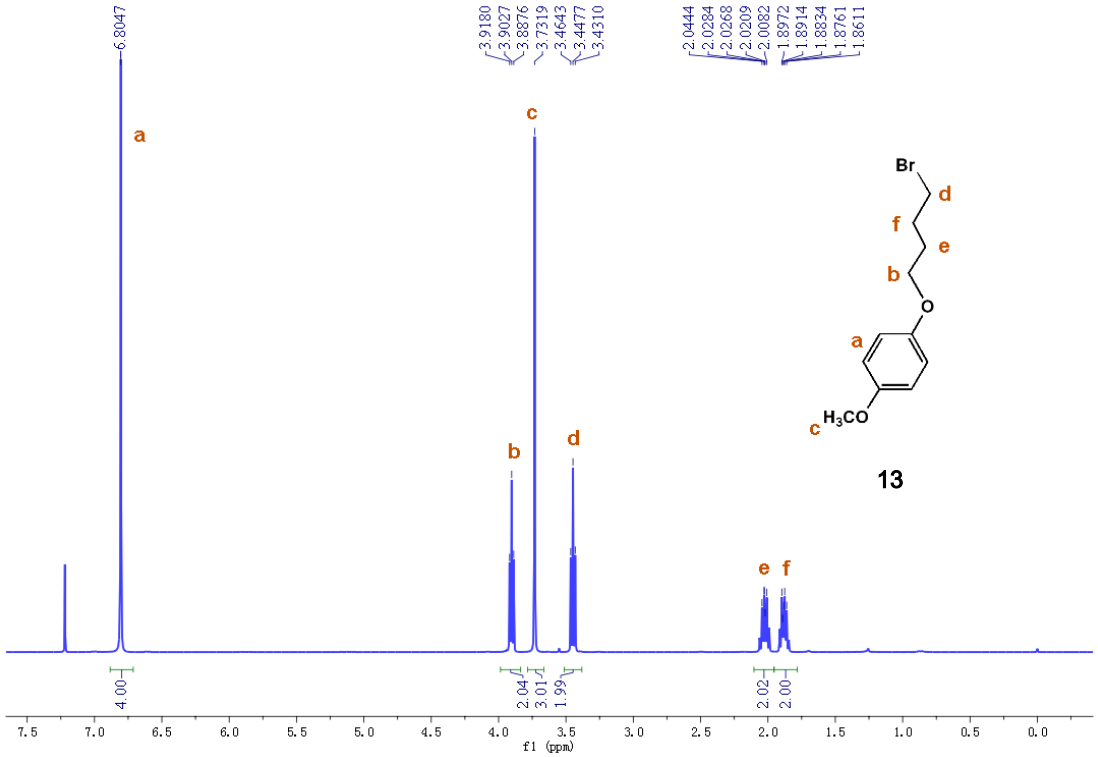

Figure S50. ^{1}H NMR spectrum (400 MHz, $CDCl_3$, 298 K) of compound **13.**

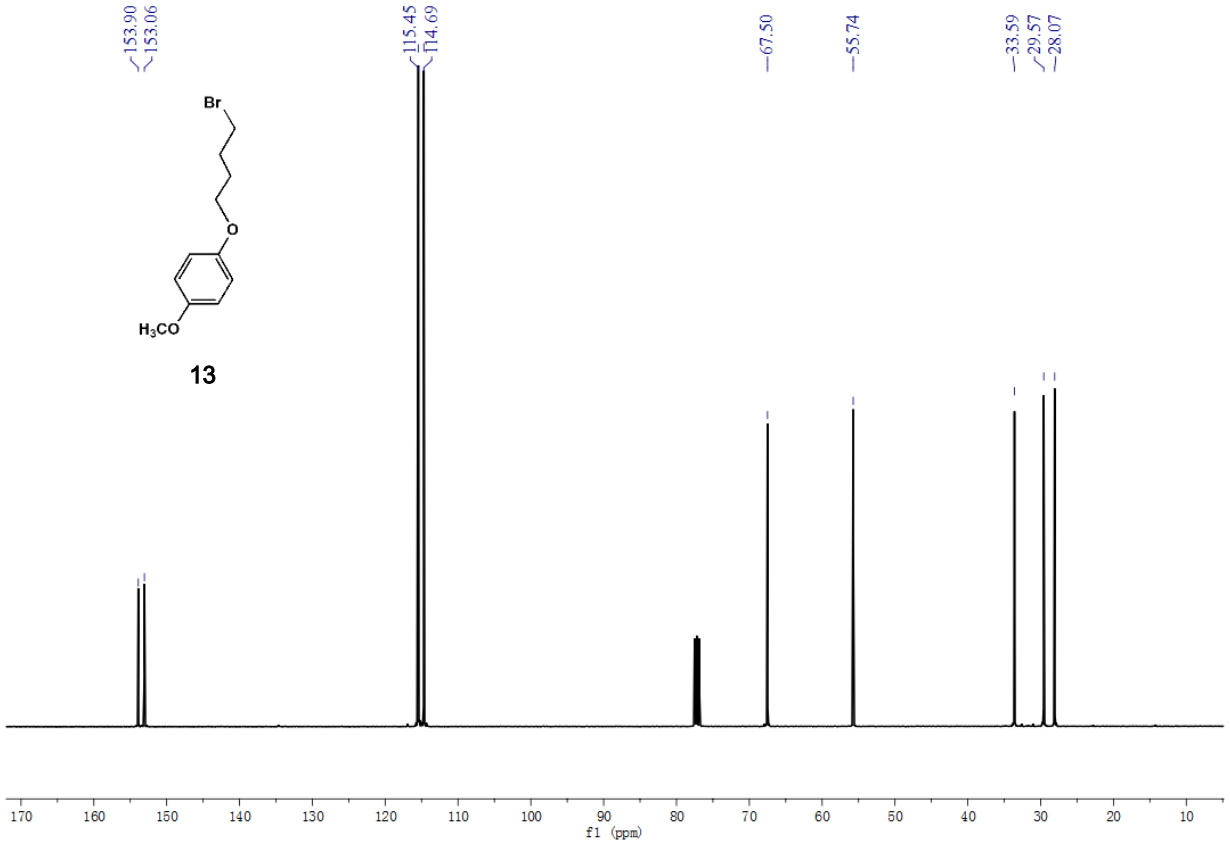

Figure S51. ^{13}C NMR spectrum (100 MHz, $CDCl_3$, 298 K) of compound **13.**

10.13 Compound **14**

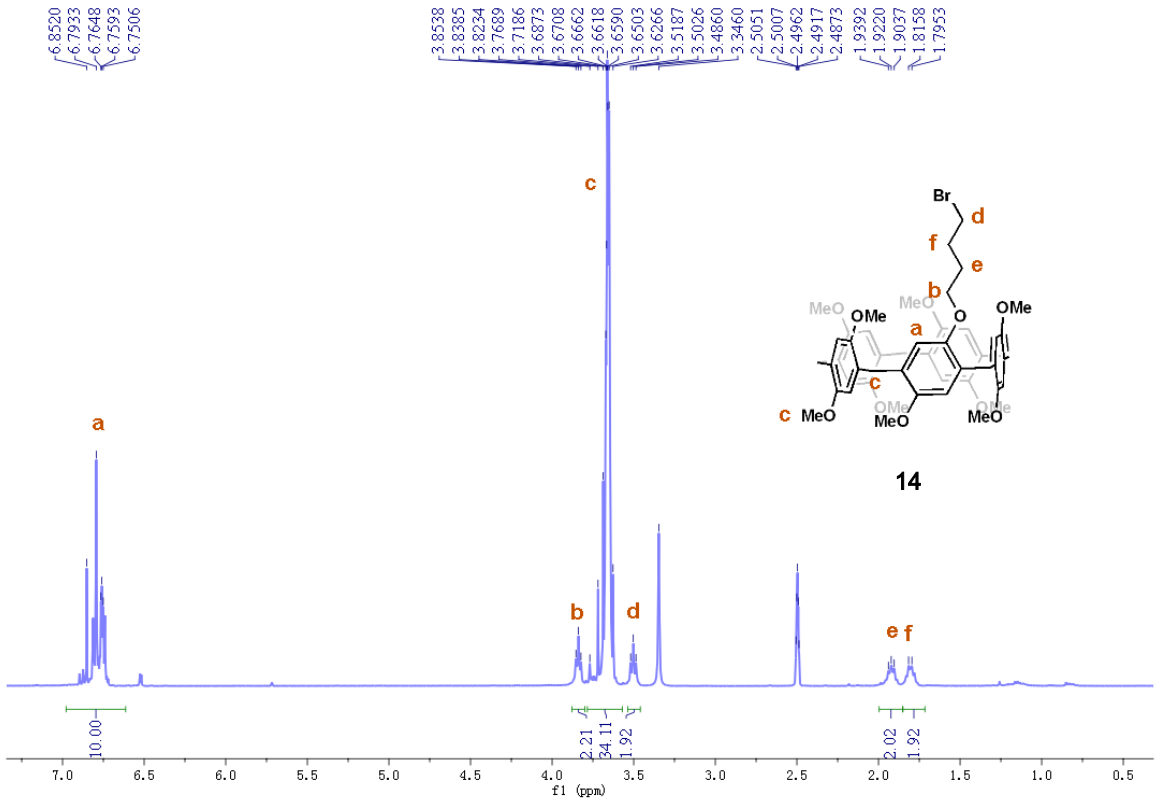

Figure S52. ^{1}H NMR spectrum (400 MHz, DMSO-d_6, 298 K) of compound **14.**

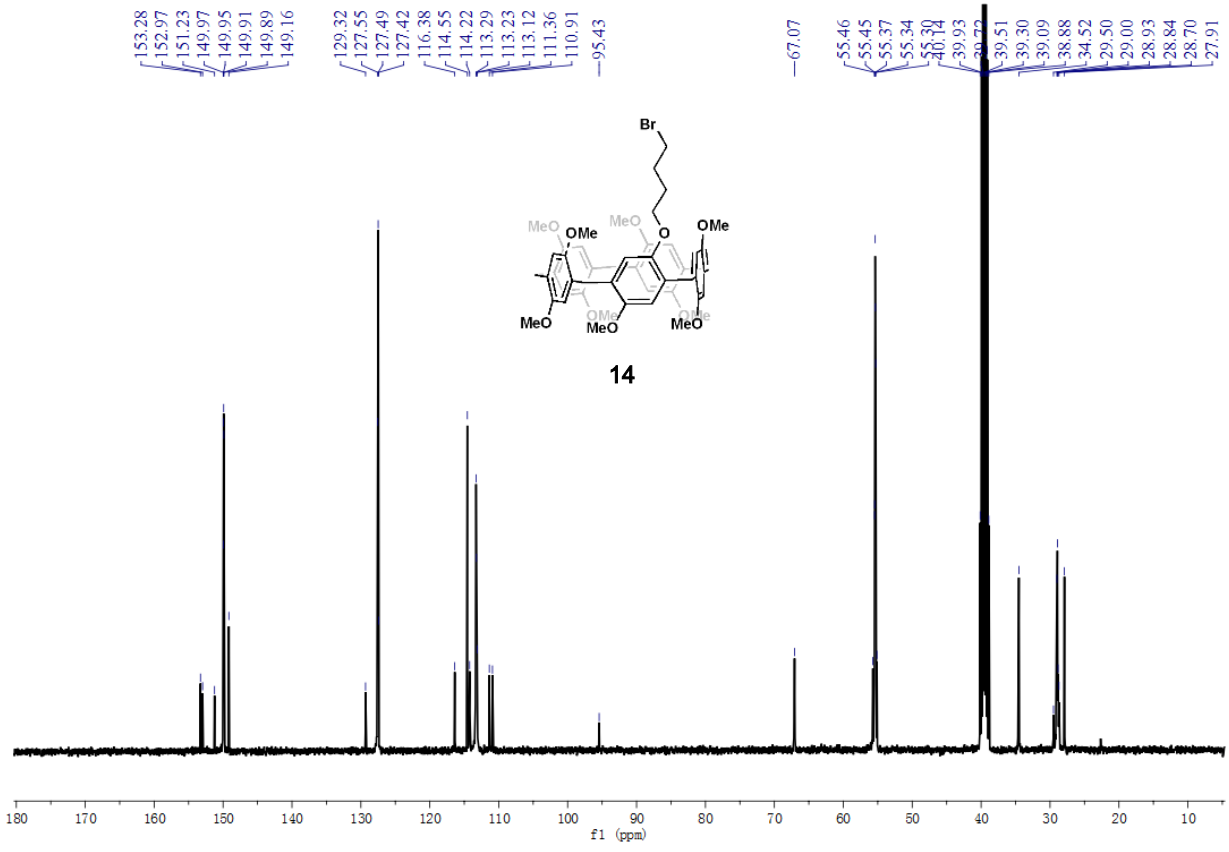

Figure S53. ^{13}C NMR spectrum (100 MHz, DMSO-d_6, 298 K) of compound **14.**

10.14 Compound **15**

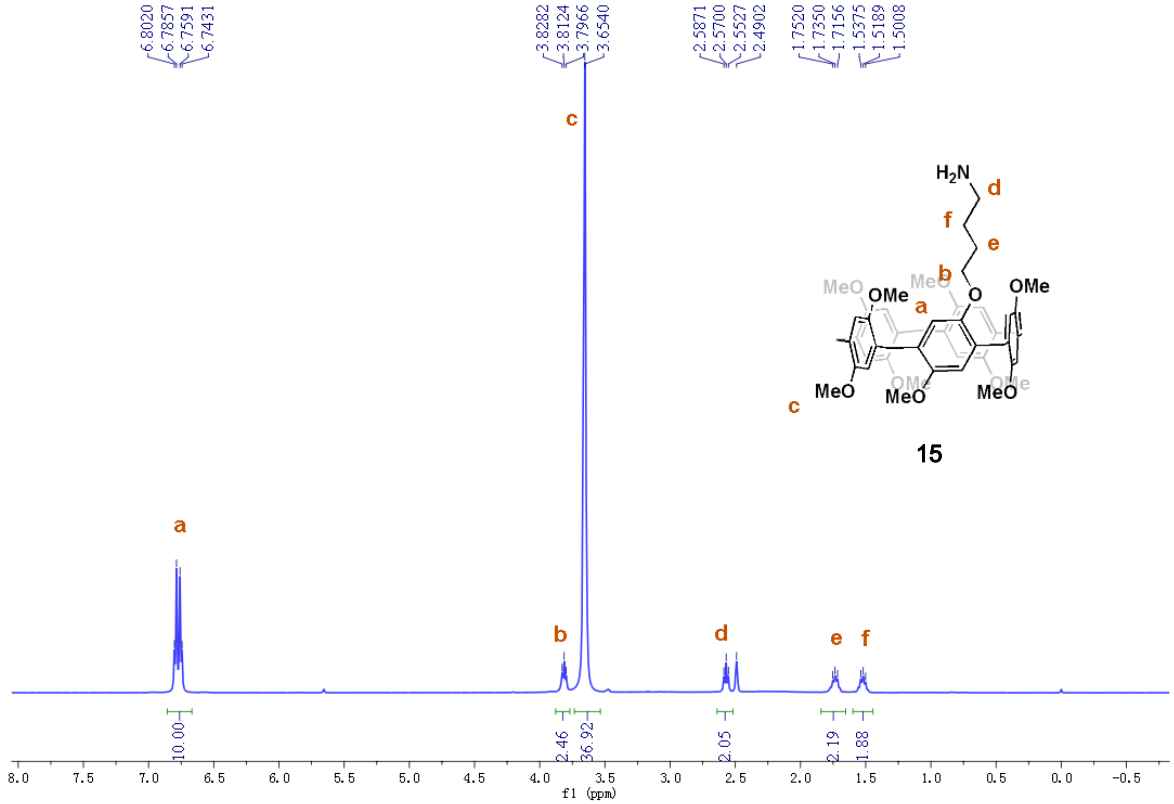

Figure S54. ^{1}H NMR spectrum (400 MHz, DMSO-d_6, 298 K) of compound **15.**

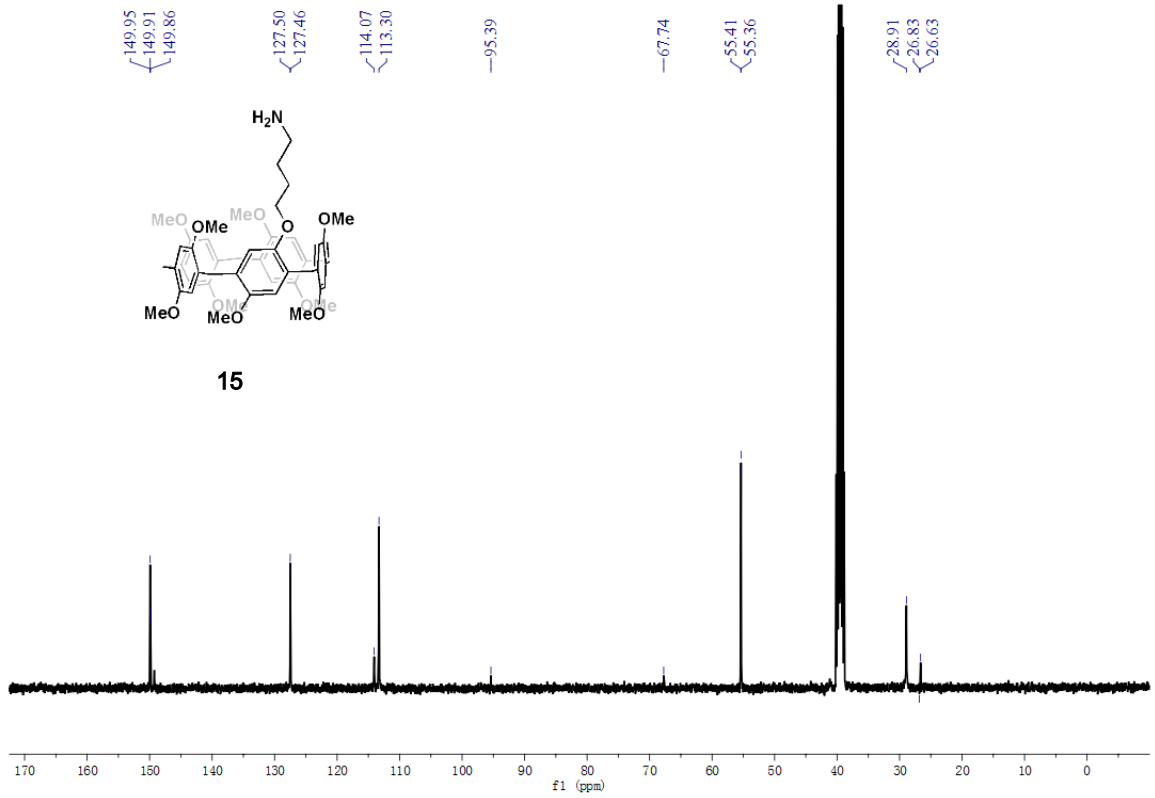

Figure S55. ^{13}C NMR spectrum (100 MHz, DMSO-d_6, 298 K) of compound **15.**

10.15 Compound **16**

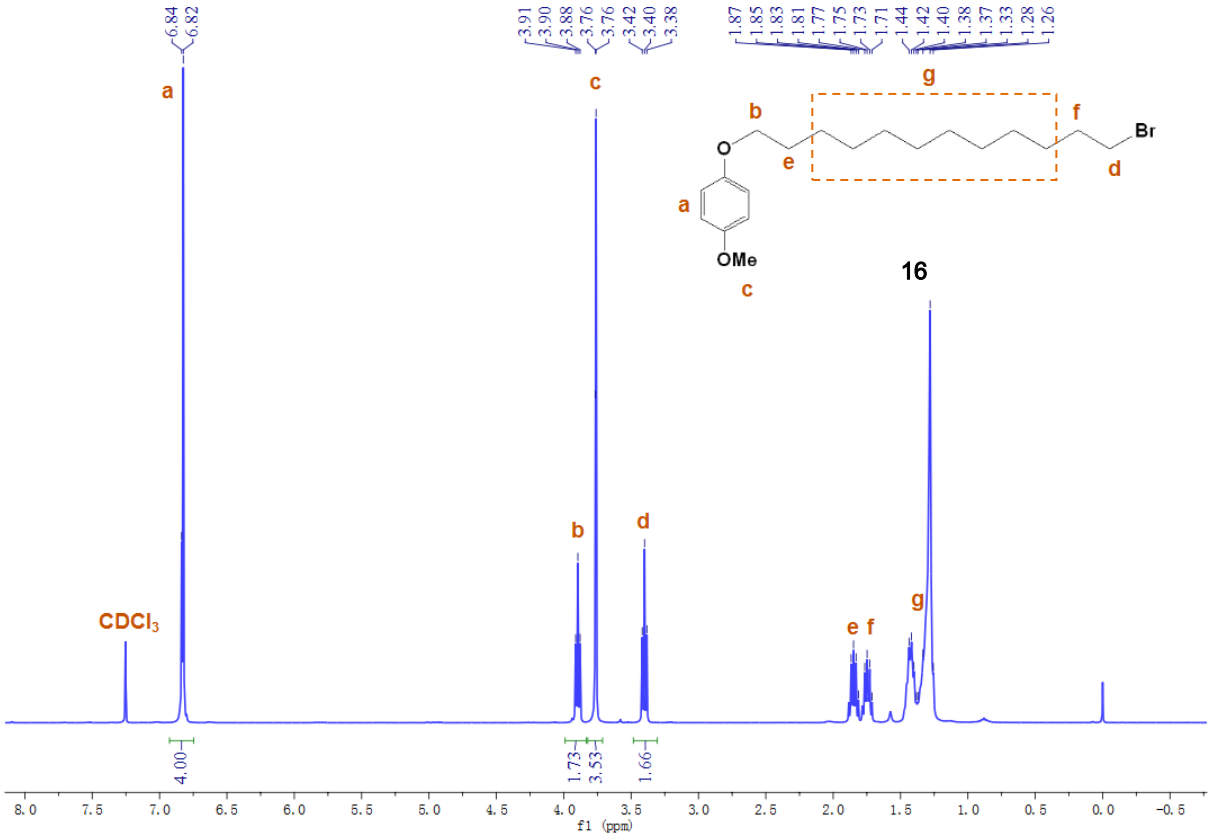

Figure S56. ^{1}H NMR spectrum (400 MHz, $CDCl_3$, 298 K) of compound **16.**

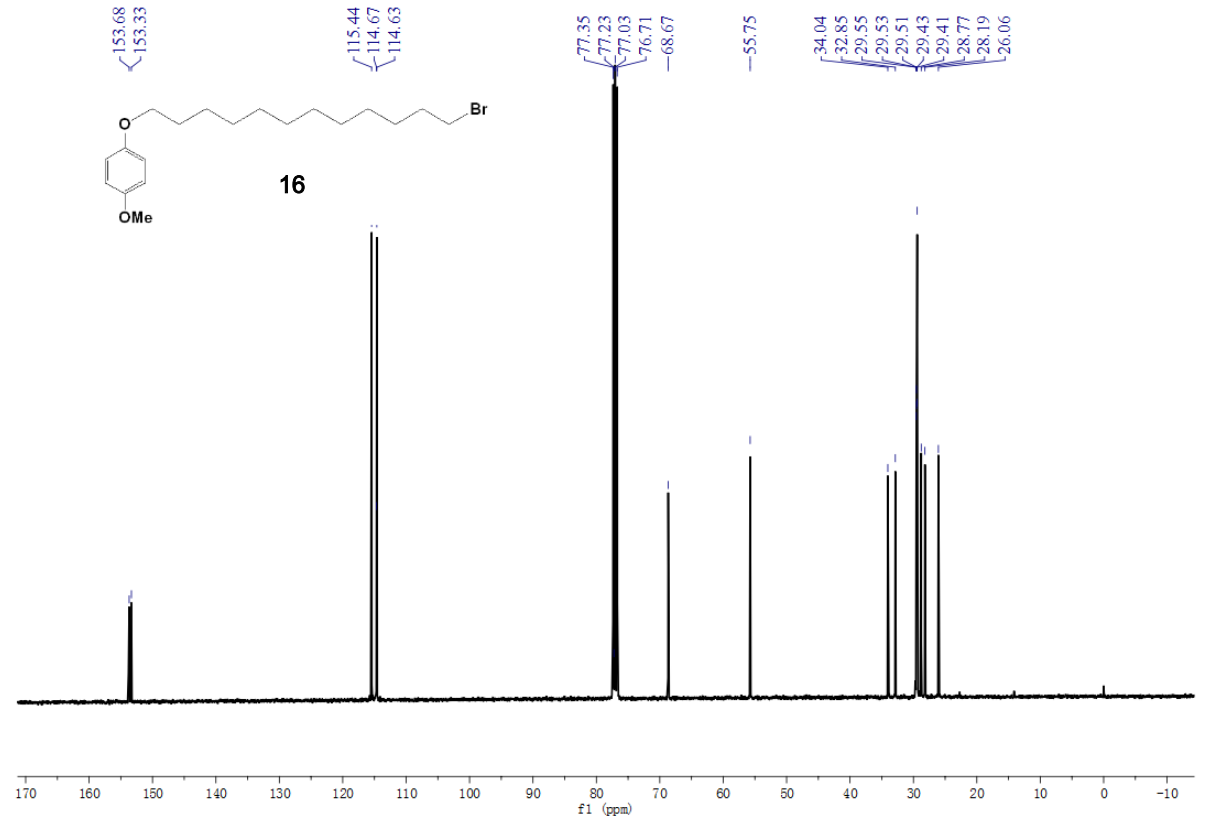

Figure S57. ^{13}C NMR spectrum (100 MHz, $CDCl_3$, 298 K) of compound **16.**

10.16 Compound **17**

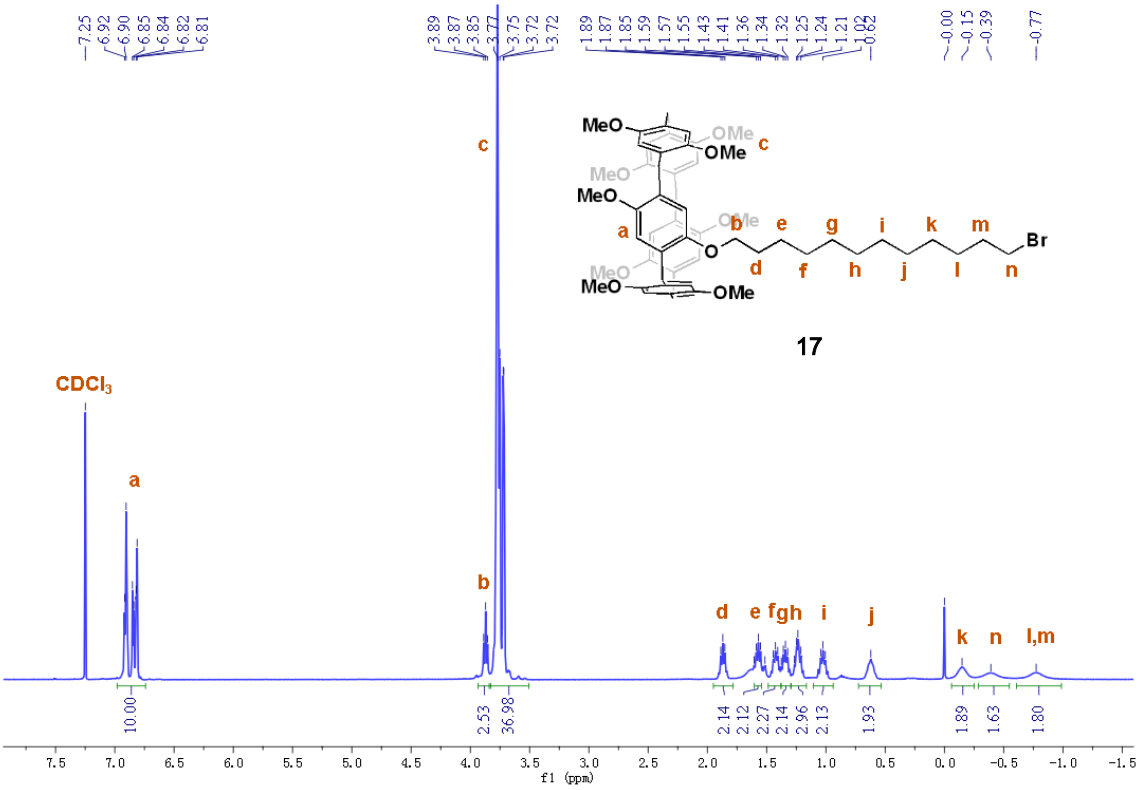

Figure S58. ^{1}H NMR spectrum (400 MHz, $CDCl_3$, 298 K) of compound **17.**

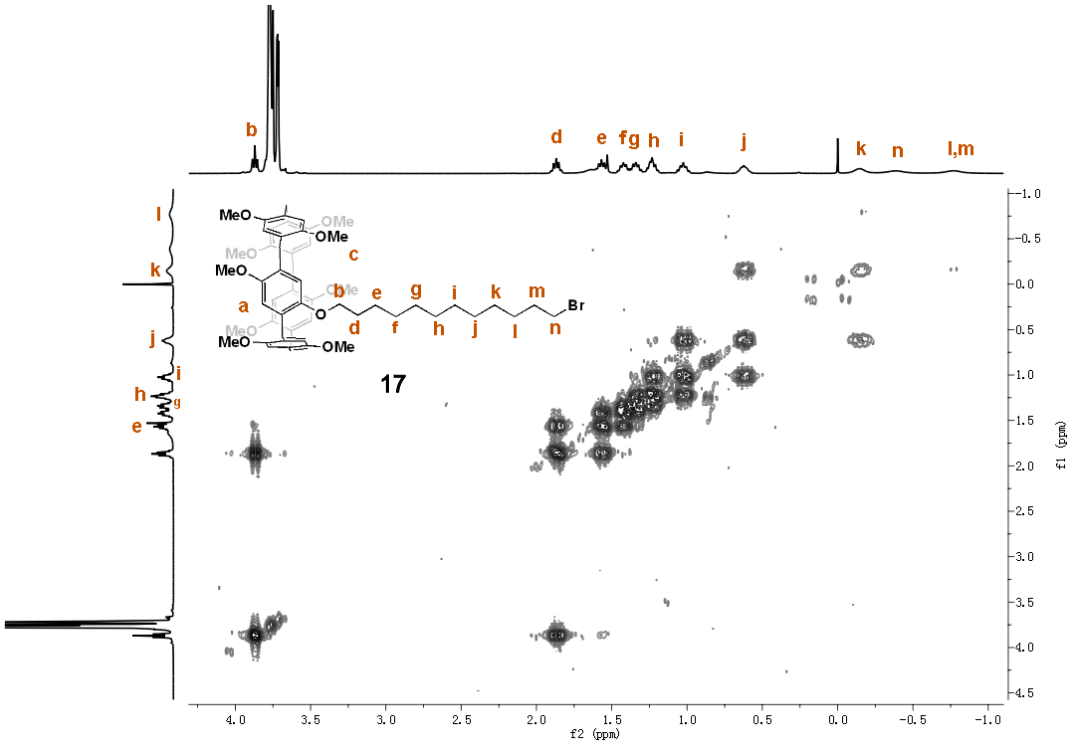

Figure S59. 2D COSY spectrum (400 MHz, $CDCl_3$, 298 K) of compound **17.**

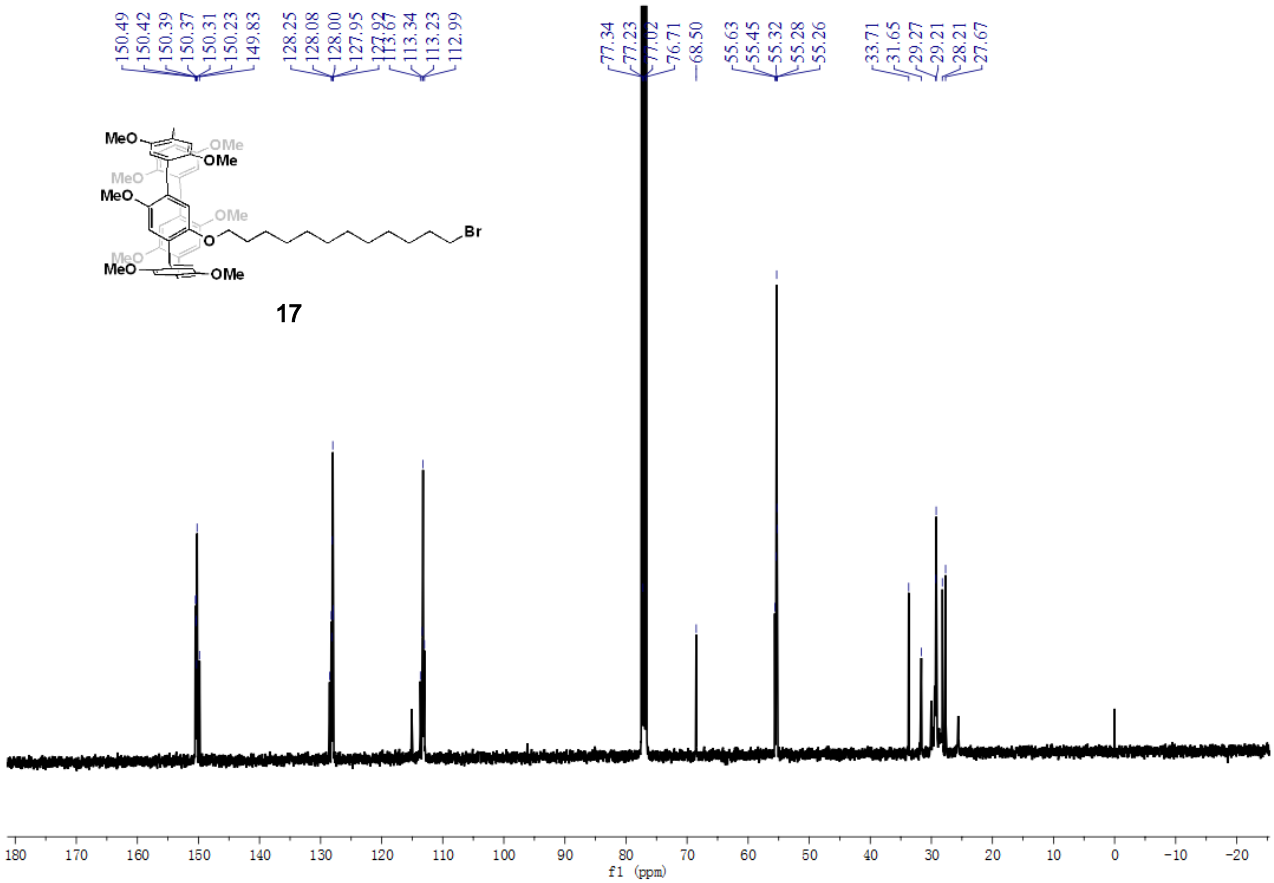

Figure S60. ^{13}C NMR spectrum (100 MHz, $CDCl_3$, 298 K) of compound **17.**

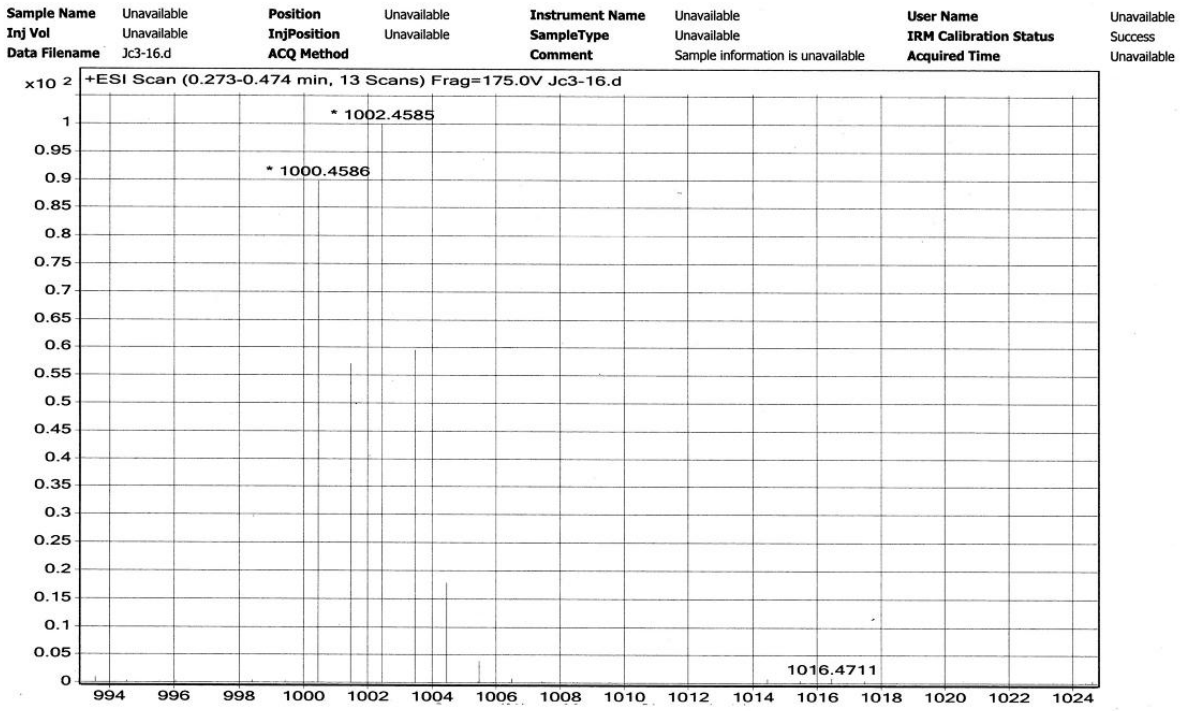

Figure S61. High resolution electrospray ionization mass spectrum of **17** (CH_3CN).

10.17 Compound **18**

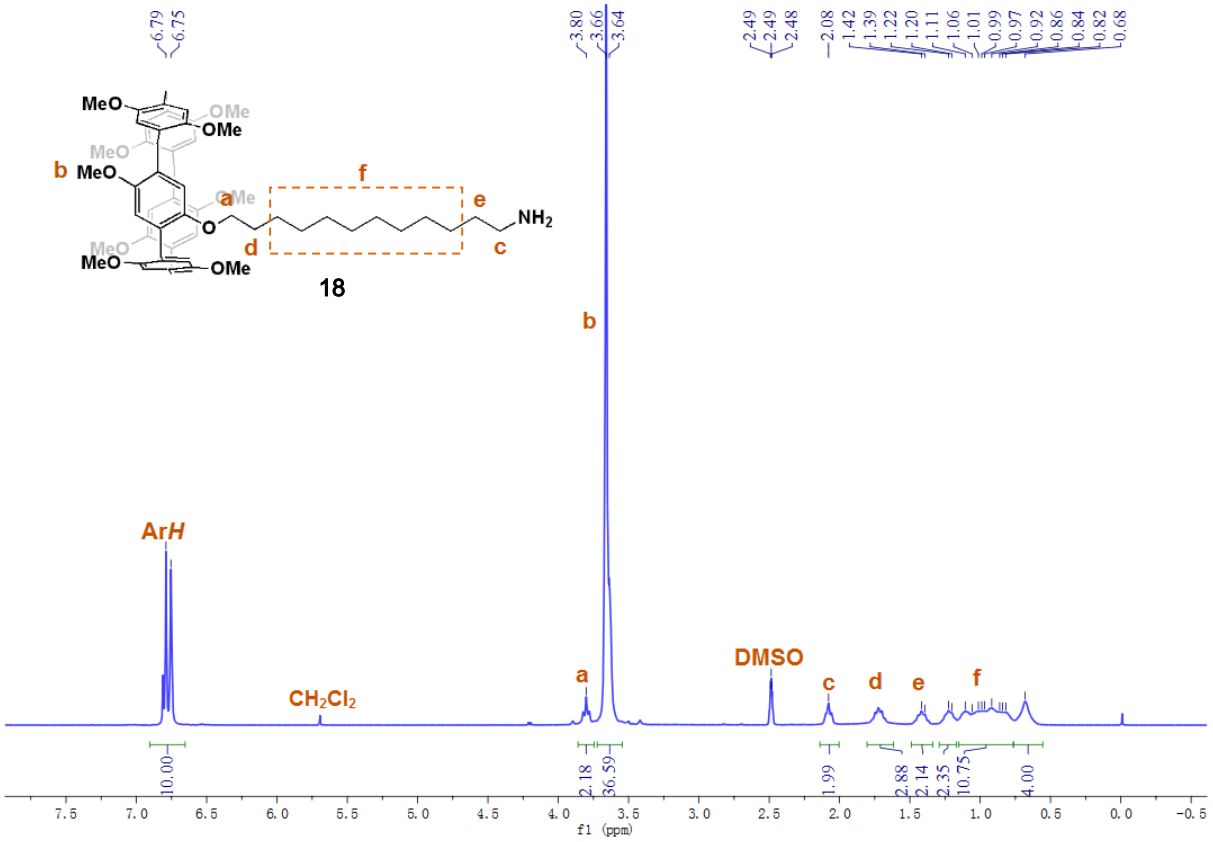

Figure S62. ^{1}H NMR spectrum (400 MHz, DMSO-d_6, 298 K) of compound **18.**

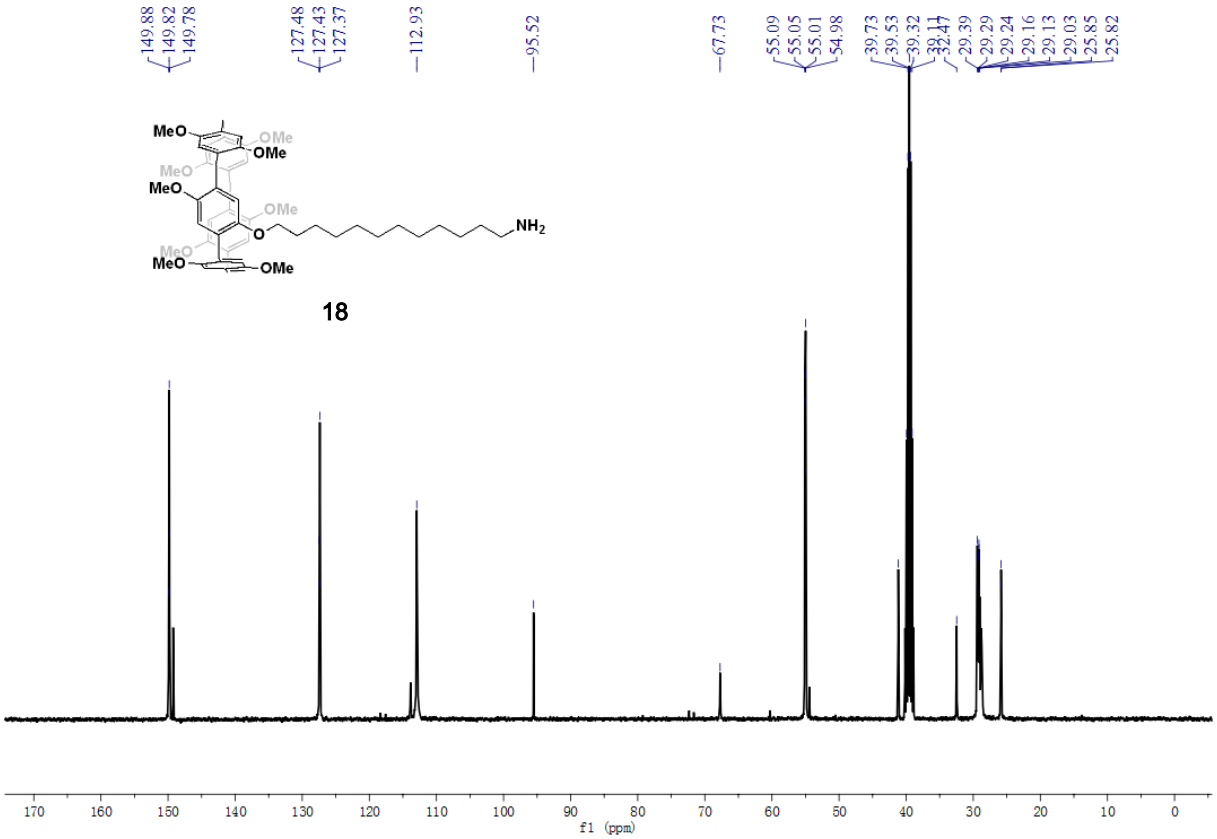

Figure S63. ^{13}C NMR spectrum (100 MHz, DMSO-d_6, 298 K) of compound **18.**

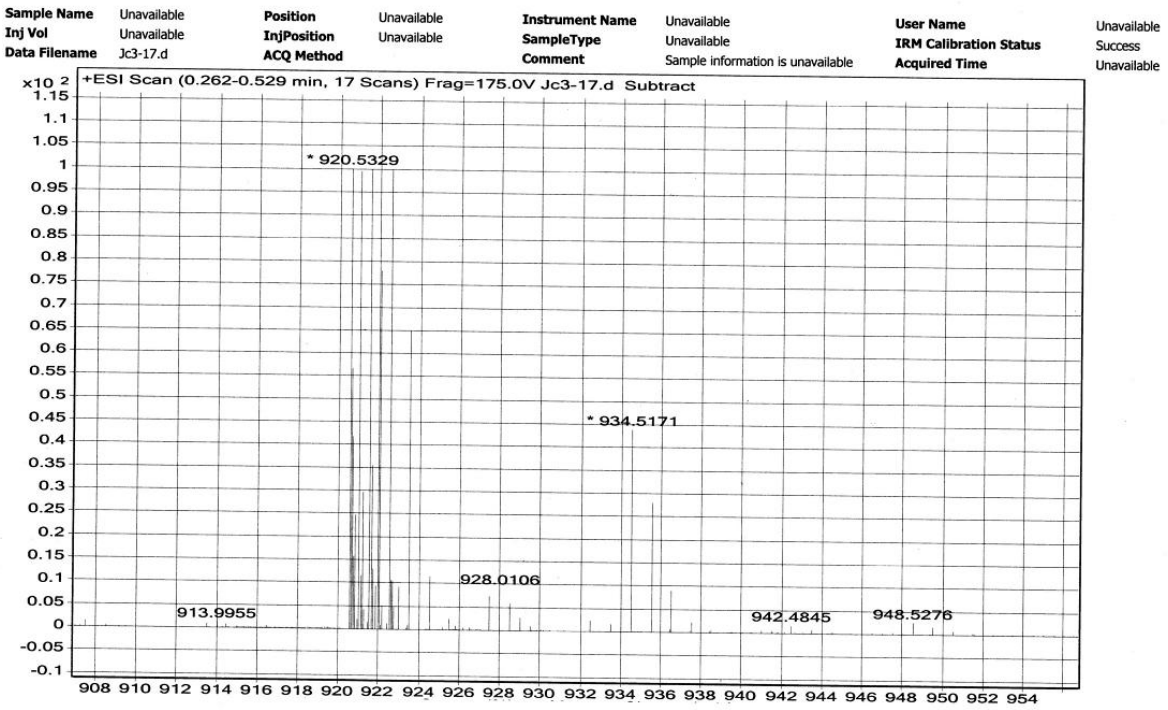

Figure S64. High resolution electrospray ionization mass spectrum of **18** (CH_3CN).

11. Theoretical Calculation

All the theoretical calculations were carried out with Gaussian 09 program package [S1] to optimize the geometries and to compute the ^{1}H NMR chemical shifts and vibrational frequencies using the DFT, M062X functional and the 6-31G (d, p) basis set.

Table S1. The calculated energies of the optimized geometries for three isomers and the energy differences based on the $\mathbf{1}_{conf1}$.

	$\mathbf{1}_{conf1}$	$\mathbf{1}_{conf2}$	**1u**
E(a.u.)	**-3474.84959**	-3474.84421	-3474.80808
△E (kcal/mol)	0.0	3.38	26.05

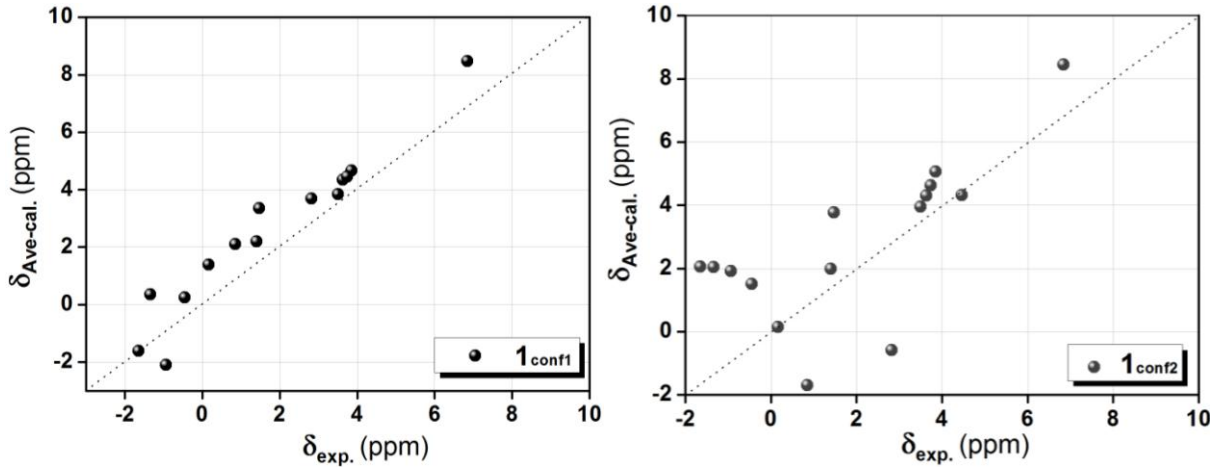

(a) (b)

Figure S65. Correlation of the experimental data with the calculated ^{1}H NMR chemical shifts based on the optimized geometries of (a) $\mathbf{1}_{conf1}$ and (b) $\mathbf{1}_{conf2}$.

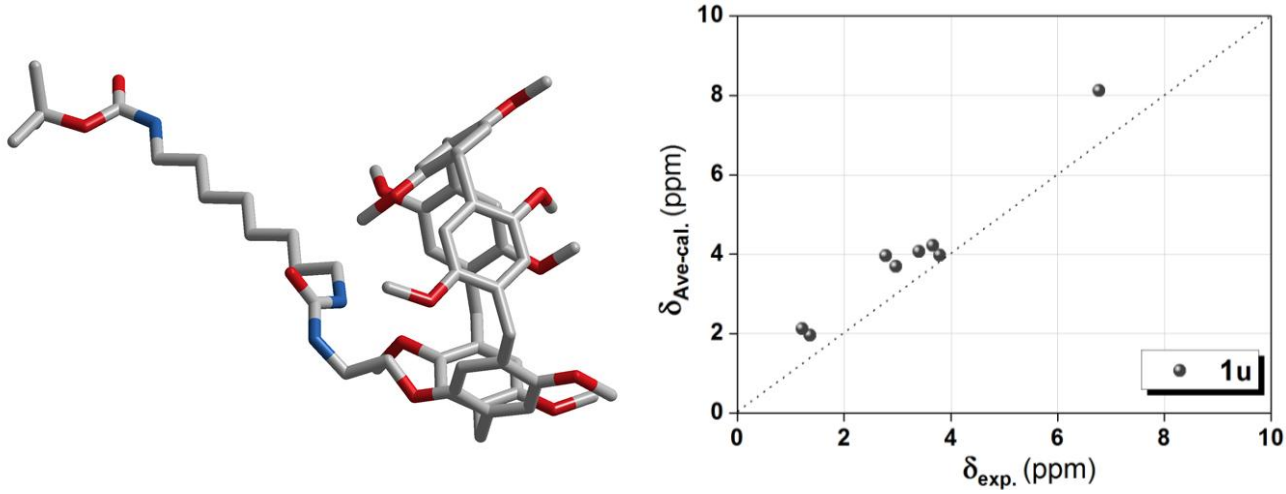

(a) (b)

Figure S66. (a) The optimized geometries of the pseudo[1]rotaxane **1u** at M062X/6-31G (d, p) level using PCM model. (b) Correlation of calculated ^{1}H NMR chemical shifts based on the optimized geometry of **1u** with the experiment.

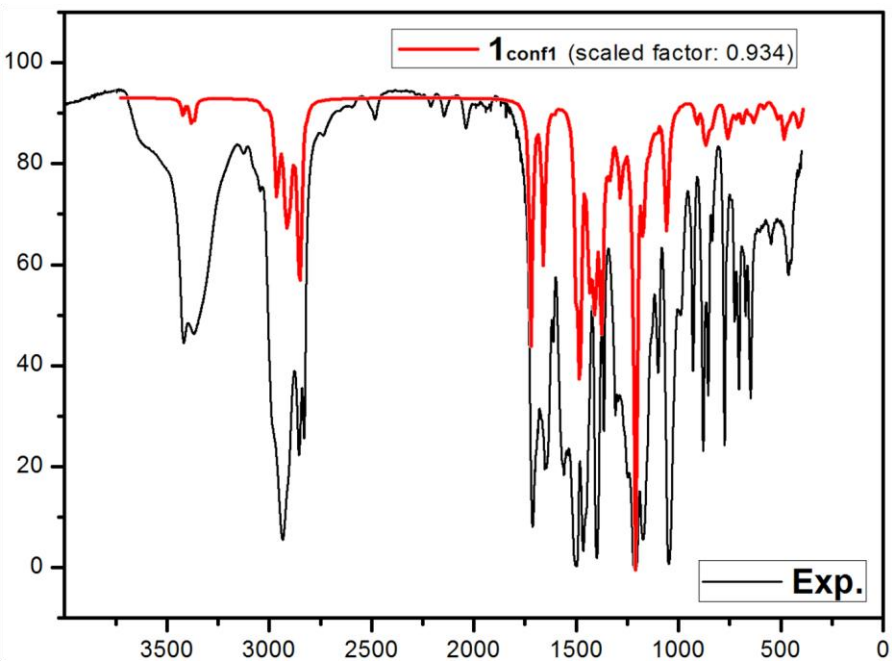

Figure S67. Comparison of the calculated infrared spectrum based on the optimized geometry of $\mathbf{1}_{conf1}$ to the experiment.

12. References

S1. Frisch, M. J.; Trucks, G. W.; Schlegel, H. B.; Scuseria, G. E.; Robb, M. A.; Cheeseman, J. R.; Scalmani, G.; Barone, V.; Mennucci, B.; Petersson, G. A.; Nakatsuji, H.; Caricato, M.; Li, X.; Hratchian, H. P.; Izmaylov, A. F.; Bloino, J.; Zheng, G.; Sonnenberg, J. L.; Hada, M.; Ehara, M.; Toyota, K.; Fukuda, R.; Hasegawa, J.; Ishida, M.; Nakajima, T.; Honda, Y.; Kitao, O.; Nakai, H.; Vreven, T.; Montgomery, J. A.; Jr., Peralta, J. E.; Ogliaro, F.; Bearpark, M.; Heyd, J. J.; Brothers, E.; Kudin, K. N.; Staroverov, V. N.; Keith, T.; Kobayashi, R.; Normand, J.; Raghavachari, K.; Rendell, A.; Burant, J. C.; Iyengar, S. S.; Tomasi, J.; Cossi, M.; Rega, N.; Millam, J. M.; Klene, M.; Knox, J. E.; Cross, J. B.; Bakken, V.; Adamo, C.; Jaramillo, J.; Gomperts, R.; Stratmann, R. E.; Yazyev, O.; Austin, A. J.; Cammi, R.; Pomelli, C.; Ochterski, J. W.; Martin, R. L.; Morokuma, K.; Zakrzewski, V. G.; Voth, G. A.; Salvador, P.; Dannenberg, J. J.; Dapprich, S.; Daniels, A. D.; Farkas, O.; Foresman, J. B.; Ortiz, J. V.; Cioslowski, J.; Fox, D. J. Gaussian 09, Revision B.01; Gaussian, Inc., Wallingford CT, 2010.